DEVELOPMENT OF PS/MMT NANOCOMPOSITE WITH IMPROVED GAS BARRIER PROPERTY

by

HUSEYIN YIGIT

Diploma work No. 67/2011
at Department of Materials and Manufacturing Technology
CHALMERS UNIVERSITY OF TECHNOLOGY
Gothenburg, Sweden

Diploma work in the Master programme Materials and Nanotechnology

Performed at: SP Technical Research Institute of Sweden
SP Technical Research Institute of Sweden, Box 857, SE - 501 15 Borås

Supervisor(s): Prof. Ignacy Jakubowicz, Dr. Jonas Enebro
SP Technical Research Institute of Sweden
SP Technical Research Institute of Sweden, Box 857, SE - 501 15 Borås

Examiner: Prof. Rodney Rychwalski
Department of Materials and Manufacturing Technology
Chalmers University of Technology, SE - 412 96 Gothenburg

DEVELOPMENT OF PS/MMT NANOCOMPOSITE WITH IMPROVED GAS BARRIER PROPERTY

HUSEYIN YIGIT

Diploma work no 67/2011
Department of Materials and Manufacturing Technology
Chalmers University of Technology
SE-412 96 Gothenburg
Sweden
Telephone + 46 (0)31-772 1000

Cover:
[Polymeric material for food packaging and its gas barrier property]

[printing office name]
Gothenburg, Sweden 2011

DEVELOPMENT OF PS/MMT NANOCOMPOSITE WITH IMPROVED GAS BARRIER PROPERTY

HUSEYIN YIGIT
Department of Materials and Manufacturing Technology
Chalmers University of Technology

ABSTRACT

Polystyrene (PS) is a versatile material and its use continuously increases in our daily life. In many applications it can be traced easily such as food packaging, domestic appliances, electronic goods, toys, household goods and furniture. One of the most important applications is considered using it as food packaging material. The need to prolong shelf life of edible products leads us to study improvement of gas permeability property in PS to meet that demand.

The aim of the present study was to prepare PS/clay nanocomposites based on commercially available constituents, using a convenient, highly efficient and feasible production method, established for traditional compounding. Ultimate goal in the following study was assigned to manufacture PS/clay nanocomposite with improved gas barrier property by melt blending using a co-rotating twin screw extruder equipped with a volumetric main and side feeder and L/D ratio 40. The effect of three different commercially available organo-modified montmorillonite (OMMT) clays was investigated for PS matrix, particularly the compatibility and improving the gas barrier property. Depending upon the exfoliation/intercalation and dispersion of layered silicates, enhancement in mechanical, thermal and optical properties was investigated. The thermal properties were investigated by thermo-gravimetric analysis (TGA) and differential scanning calorimetry (DSC) while the morphology and dispersion of the clay in the polymeric matrix in the masterbatches and composite materials were investigated using wide angle X-ray diffraction (WAXD) and high resolution scanning electron microscopy (HR-SEM) respectively. Interlayer distance and intercalation of the modified clays in masterbatches were determined by WAXD. The mechanical properties were analyzed by tensile tests and the optical properties by ultraviolet visible (UV/VIS) spectrometry. The oxygen gas permeability was tested by a gas permeability tester.

It was concluded that the attempted nanocomposite fabrication resulted in microcomposite formation, nevertheless some enhancement in properties was achieved. When compared with unfilled PS, gas barrier property increased by 25% and 27% for PS/Dellite 67G, PS/Nanofil SE 3010 and by 15% for PS/Cloisite 11B. Increase in thermal decomposition temperature by 20^{o}C, for all materials, was obtained. The Young's modulus for the three composites practically remained unchanged. The glass transition temperature (T_g) was affected slightly, in the following way: for the PS/clay microcomposites prepared with Dellite 67G and Nanofil SE 3010 clays, an increase by 2^{o}C was found, while PS/Cloisite 11B microcomposite, a decrease by 2^{o}C in T_g was found. Prepared materials displayed reduction in transmittance by 27%, 37% and 11% in UV/VIS region (200-800nm) for PS/Dellite 67G, PS/Nanofil SE 3010 and PS/Cloisite 11B, respectively. The elongation at break and tensile strength showed decreasing values by 16.7% and 9.5% for PS/Nanofil SE 3010 and 15.0% and 14.1% for PS/Cloisite 11B respectively while these values were not claimed for PS/Dellite 67G owing to fracture of the specimens took place in measurement section.

Keywords: Nanocomposite, polystyrene, gas barrier, melt blending, MMT

ACKNOWLEDGEMENT

This project is entirely dedicated to **my family**. Without their continuous support and trust this endeavor would not come to an end.

Especially, I would like to thank to **my brother Cengiz Yigit** and **my girlfriend Galina Shavard** for having endless faith in me.

I would like to thank to my supervisors at **SP Technical Research Institute of Sweden Prof. Ignacy Jakubowicz** and **Dr. Jonas Enebro** whose profound knowledge, creative attitude and support made my project invaluable. His guidance throughout the project was worthwhile experiencing at **SP**. I have equipped in many ways in his presence. I gained new vision and I have now better understanding after working with him.

I admit myself lucky to have friends like **Peter Löwenhielm, Kenneth Möller, Elva Peterson, Linda Eriksson, Haleh Yaghooby Shahrestani** and to have their contribution and interests in my project. I also would like to thank to **Prof. Vratislav Langer** for helping me in WAXD analysis, **Prof. Rodney Rychwalski** for being my examiner and **all my professors** in the university.

I am glad to know department of **KMp crew** at **SP**. It was pleasure to work in the presence of each of them.

I appreciate **Laviosa, Southern Clay, and Nanocor companies** supplying materials for my project.

TABLE OF CONTENTS

LIST OF ABBREVIATIONS AND SYMBOLS

ABS,	Acrylonitrile-Butadiene-Styrene
Al,	Aluminum
Al^{3+},	Aluminum Ion
Ar,	Argon
C,	Carbon
^{o}C,	Degree Celcius (Centigrade)
CEC,	Cation Exchange Capacity
cm,	Centimeter
CO_2,	Carbon dioxide
Cs,	Cesium
d,	*d-spacing* (Interlayer Distance)
D,	Diameter
DSC,	Differential Scanning Calorimetry
E-Modulus,	Young`s Modulus (Tensile Modulus)
Fe,	Iron
g,	Gram
GPa,	Gigapascal
GPPS,	General Purpose Polystyrene
H,	Hydrogen
H_2O,	Water
He,	Helium
HIPS,	High Impact Polystyrene
HRR,	Heat Release Rate
HR-SEM,	High Resolution Scanning Microscopy
K^+,	Potassium Ion
kN,	Kilonewton
kV,	Kilovolt
L,	Length
Li,	Lithium
LS,	Layered Silicate
M,	Monovalent Cation
m,	Meter
mA,	Miliamper
MA,	Methacrylate
mbar,	Milibar
meq,	Miliequivalent
Mg,	Magnesium
Mg^{2+},	Magnesium Ion
min,	Minute
ml,	Mililiter
mm,	Milimeter
MMA,	Methyl Methacrylate
MMT,	Montmorillonite
MPa,	Megapascal
MTS,	Mica Type Layered Silicate
N,	Newton
N_2,	Nitrogen gas
N6,	Nylon-6

n_m, n_p,	Refractive Index
Na,	Sodium
Na^+,	Sodium Ion
Na^+ MMT,	Sodium Montmorillonite
nm,	Nanometer
O,	Oxygen
O_2,	Oxygen gas
OH,	Hydroxyl
OMMT,	Organo Modified Montmorillonite
OTR,	Oxygen Transmission Rate
PEO,	Poly(ethylene oxide)
PLSN,	Polymer Layered Silicate Nanocomposite
PMMA,	Poly(methyl methacrylate)
PP,	Polypropylene
PS,	Polystyrene
PVA,	Poly(vinyl alcohol)
PVC,	Polyvinyl chloride
PVP,	Poly(vinyl pyrrolidone)
Rb,	Rubidium
RH,	Relative Humidity
RI,	Refractive Index
rpm,	Revolutions per minute
sec,	Second
SAXS,	Small Angle X-ray Scattering
Si,	Silicon
Si^{4+},	Silicon Ion
T_g,	Glass Transition Temperature
TEM,	Transmission Electron Microscopy
TGA,	Thermo-gravimetric Analysis
UV/VIS,	Ultraviolet Visible
WAXD,	Wide Angle X-ray Diffraction
wt,	Weight
x,	Degree of Isomorphous Substitution
XRD,	X-ray Diffraction
Å,	Angstrom
Δ,	Heat
λ,	Lambda
µm,	Micrometer

LIST OF FIGURES

LIST OF TABLES

1. INTRODUCTION

Layered clay composites (modified or not) in nanometer scale has drawn special attention [1] since the engineering properties of polymer clay nanocomposites exhibit outstanding improvements in performance properties when compared to either virgin polymers or conventional composites. These improvements include enhanced tensile strength, tensile modulus, flexural strength and modulus, heat distortion temperature [2] improved gas barrier properties, reduced flammability [3]. In such nanocomposites, the interfacial interaction between silicate clays and polymer matrix plays key role for the desired outcomes in small amount of clay loading typically 3-5 %.

Regarding the facts that in this project, the objective is assigned to prepare PS/clay nanocomposites with enhanced gas barrier, mechanical, thermal and optical properties by melt blending process using different commercial available organo modified clays.

1. 1. POLYSTYRENE

PS is a thermoplastic polymer with the repeating unit shown in Figure 1. Just as polypropylene (PP), polyvinyl chloride (PVC) and other vinyl compounds, various stereo-regular forms of PS are possibly present [4]. The benzene ring present in the PS structure diminishes the ability of polymer chain to bend and interact with other parts of the molecule. Owing to these characteristics, no crystallization takes place hence PS is considered 100% amorphous polymer. Moreover, this large side group randomly distributed in the structure prevents crystallization to take place as well as increases tensile strength. Normally tensile strength is related to crystallinity and higher molecular weight but PS also demonstrates high tensile strength due to size of pendant group causing steric effect. In the case, one pendant group on a chain in PS prevents movement of other pendant group on another chain. These interactions among pendant groups promote disentanglement of polymer chains not to slide past each other thus increase in tension is simply pronounced. However, PS is quite brittle due to restriction in movement of polymer chains caused by large aromatic groups. Therefore PS is not easily capable of absorbing sudden impacts [5].

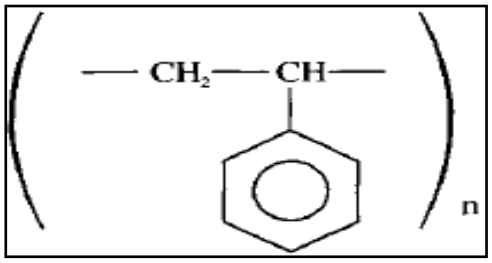

Figure 1: Polystyrene (PS) polymer repeating unit [4].

PS is known as hard rigid transparent thermoplastic and it is considered free from odor and taste. When it is burned, it releases yellow flame with a dark, sooty smoke and it has a low density. It is generally used as injection molding and vacuum forming material since it is advantageous to utilize its low cost, low moisture absorption, good dimensional stability, good

electrical insulation, colourability and reasonably chemical resistance. The main drawbacks with PS are considered its brittleness, low profile to withstand temperature of boiling water and average oil resistance [4]

Mechanical properties of PS are rather dependent upon the nature of the polymer e.g. its molecular weight, method of sample preparation for testing [4] while chemical properties of PS determined largely by the pendant group. Any molecule containing benzene ring has certain chemical properties. These properties can be considered sensitivity towards aromatic and chlorinated solvents. Therefore PS is susceptible to dissolve in these solvents However, PS is resistant to water and has been used extensively for applications such as food packaging [5]. Another outstanding property of PS is its optical property. PS is highly transparent and clear, since amorphous nature of PS allows the transmission of all wavelengths of visible light without significant refraction [4].

1. 2. POLYMER CLAY NANOCOMPOSITE

Research efforts on polymeric nanocomposites prepared with layered silicates have been drawing significant attention during last two decades due to great enhancement of properties at very low volume fractions of filler. Advantage of using low amount of filler can also be said to retain the optical clarity as well as low density of the formed composite materials. The nanocomposites are considered new class of materials which are distinguished from their counterparts conventional microcomposites. The difference between nanocomposites and microcomposites can be easily realized from the interaction of polymer matrix and inorganic filler. Crucial part in nanocomposite material is considered by the interface between the organic and inorganic phases due to dispersion of inorgnic filler particles in nanoscale range in polymer matrix. This enormous interaction of the two constituents of the composite leads to different morphology at the interface whose properties are markedly different from bulk polymer. These contacts between polymer matrix and inorganic phases promote improvement in mechanical, thermal and gas barrier properties for better load transfer, better heat transfer to the inorganic part that acts as insulator and mass transport barrier material, and longer pathway for the gas molecules which penetrate through the composite thus creating barrier resistance respectively. This synergistic improvement in the properties of the composites makes them highly potential materials to use in many various applications. Aspect ratio, volume fraction, geometry, alignment and state of exfoliation in organic phase remarkably affect the properties of formed composites. For instance, polymer nanocomposites are generally prepared for the improvement of mechanical performance hence allowing their use as engineering materials [6]. In particular, driving force leading to extensive researches on this area was the study stimulated by the Toyota research group. In the work of the group nylon-6 (N6)–montmorillonite (MMT) nanocomposite was commercialized. With only a small MMT loading (4.2 wt.%), the modulus doubled, the tensile strength increased more than 50%, the heat distortion temperature increased by 100^{o}C, and combustion heat release rate decreased by up to 63% [7]. However, despite the other properties have been studied in these nanocomposites, gas barrier properties have been mostly disregarded. Generally, it is considered that once the improvement on mechanical properties is achieved, this will be expected to lead to improvement in the other properties, but this may be misleading to a researcher in all cases since the barrier properties are highly dependent upon

interaction of the polymer matrix and inorganic filler. It is quite possible that mechnical performance is increased while barrier properties are reduced. When the incompatibility takes place at the interface of the polymer matrix and inorganic filler, this may lead to generation of micro voids or area with high free volume causing the extention in gas permeation throughout the composite materials as a function of filler voume fraction whereas improvement in mechanical properties can be still pronounced. Therefore, it is substantially important to develop nanocomposites with improved gas barrier property. Thus increase in barrier can extend the use of the nanocomposites in a number of applications [6].

1. 2. 1. Structure and Properties of Clay

Most commonly used type of layered silicate is montmorillonite (MMT) natural smectic clay 2:1 phyllosilicate [8]. Hectorite and saponite are also classified as layered silicates [9]. Owing to high surface area and aspect ratio, MMT clays are of special interest [10] for preparing nanocomposites. The structure of MMT consist of stack of crystalline sheets [11]. Crystal lattice of these sheets comprises two-dimensional layers where octahedral layer of aluminum or magnesium is surrounded by two external tetrahedral layers (2:1) [12]. The thickness of each sheet is considered around 1 nanometer (nm) [9] while the lateral dimension of individual layers may differ from 30 to 2000 nm depending on the particular silicate [13]. Stack of platelets is held together by electrostatic forces with interlayer distance called *d-spacing* [14] between the platelets. The interlayer is also characterized by negative surface charge [9] where counterions are attracted to the net negative charge within the clay platelets. The exchange of simple inorganic cations is very much depended upon surface charge density which is known as cation exchange capacity (CEC) expressed by meq/100g [12]. Localization of negative charge is not constant and may vary from layer to layer. Therefore, it is beneficial to consider CEC as an average value of entire crystal [9].

Generally, MMT is represented with the chemical formula $[M_x(Al_{4-x}Mg_x)Si_8O_{20}(OH)_4]$ where M refers to monovalent cation X is the degree of isomorphic substitution and silicate layers having exchangeable cations inside. Isomorphous substitution of these cations inside the galleries generates negative charge on the silicate surfaces i.e. substitution of cations such as Al^{3+} by Mg^{2+} or Si^{4+} by Al^{3+} creates a net negative charge in the gallery [12] and this charge deficiency is counterbalanced by counter ions alkali or alkaline earth metal cations throughout the gallery [10]. Structure of MMT is given in Figure 2 and chemical formulas of some layered silicates are shown in Table 1.

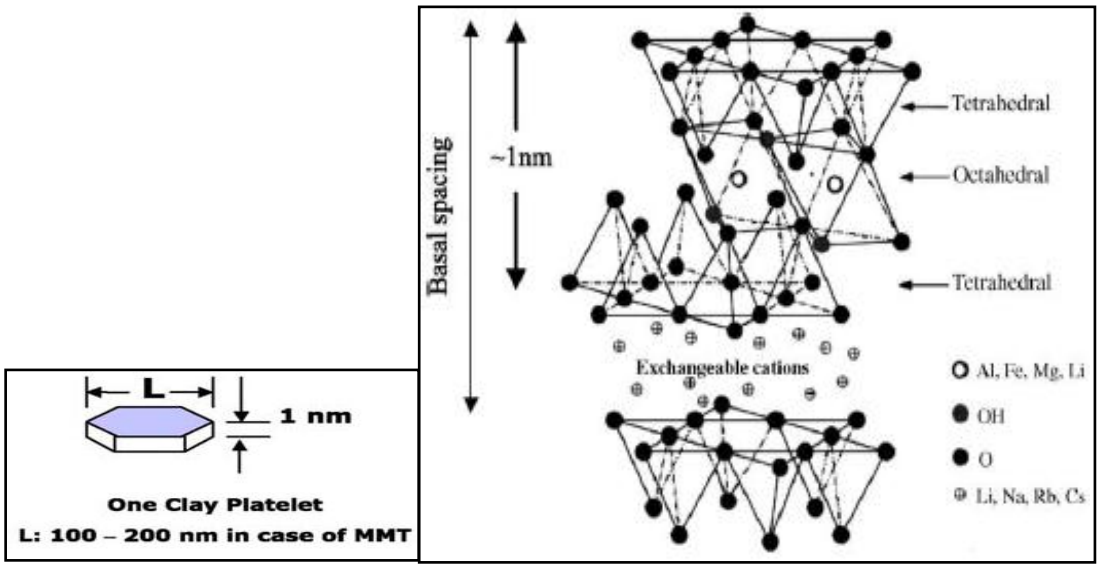

Figure 2: Structure of 2:1 phyllosilicates [15].

Table 1: Chemical formula and characteristic of commonly used clays [15].

2:1 phyllosilicates	Chemical formula	CEC (meq/100 g)	Particle length (nm)
Montmorillonite	$M_x(Al_{4-x}Mg_x)Si_8O_{20}(OH)_4$	110	100–150
Hectorite	$M_x(Mg_{6-x}Li_x)Si_8O_{20}(OH)_4$	120	200–300
Saponite	$M_xMg_6(Si_{8-x}Al_x)Si_8O_{20}(OH)_4$	86.6	50–60

M, monovalent cation; x; degree of isomorphous substitution (between 0.5 and 1.3).

1. 2. 2. Structure and Properties of Organo Modified Clay

The crucial part for better dispersion in nanocomposites is to ensure good compatibility between silicate layers and polymer matrix [14]. Generally, mixture of virgin polymer with pristine MMT, two separate phases are observed similar to immiscible polymer blends. In immiscible systems referring to conventional filled polymers such as microcomposites, poor physical interaction occurs between polymer and filler resulting in no improvements in mechanical and thermal properties. However, unlike counterparts of microcomposites strong interaction between organic polymer and inorganic layered silicate (LS) filler leads to good dispersion of LS in nanometer level in the polymer matrix showing remarkable improvements in aforementioned properties [16].

Since pristine LS contains hydrated ions such as Na^+ or K^+ ions in the gallery [17] they are considered as hydrophilic fillers. Due to this nature of LS they are compatible and readily to interact with some hydrophilic polymers such as poly(ethylene oxide) (PEO) or poly(vinyl alcohol) (PVA) or poly(vinyl pyrrolidone) (PVP) [18]. Since most of the polymers are hydrophobic that is why it is vitally important to render hydrophilic nature of LS to organophilic status in order to achieve compatibility with most of the thermoplastics and engineering polymers [14]. Generally, this modification of the surface is achieved by exchanging interlayer cations with cations bearing long alkyl chains [19] such as alkylammonium or alkylphosphonium cations [20]. These alkyl chains can bear functional groups that can either

react with polymer matrix or start in-situ polymerization [21]. That modification results in decrease in surface energy of the clay [10] allowing polymer intercalate inside the gallery. By length of alkyl chain its functionality, packing density and *d-spacing* can be manipulated for optimization of interaction between given polymer and LS. [20]. In Figure 3 schematic representation of different types of intercalation of LS by modifiers is shown.

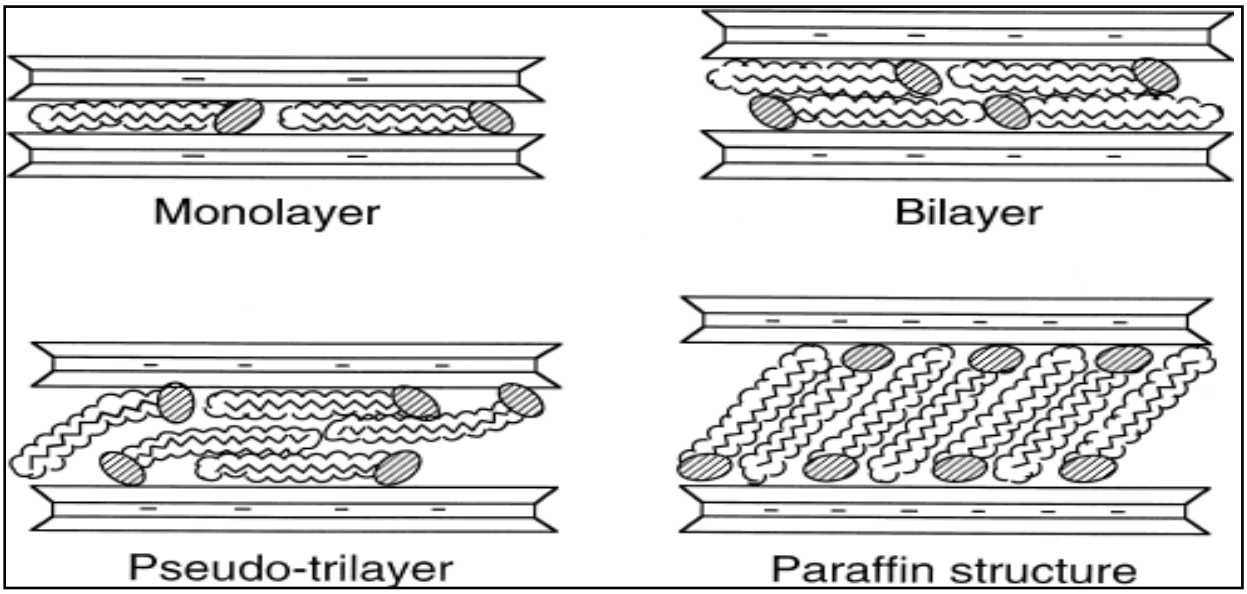

Figure 3: Orientations of alkylammonium ions in the galleries of layered silicates with different layer charge densities [22].

1. 2. 3. Types of Nanocomposites

In general, the thickness of the silicate sheets is around 1 nm [11] with high aspect ratio 10-1000 nm. That is why LS is of great interest since they offer high surface area [23]. In order to achieve evenly dispersed polymer layered silicate nanocomposite (PLSN) high surface area in the clay is required to create proper interfacial interaction throughout the polymer matrix as compared to conventional composites. Depending on the interfacial interaction between two constituents, desirable PLSNs can be attained. In this respect, three types of composite can be obtained in the presence of small loadings of the LS. These can be listed as follows.

Exfoliated nanocomposites: In this type of nanocomposite, registry between the clay sheets is lost [24] individual silicate layers are completely delaminated and dispersed in polymer matrix [13] leading to enhanced properties.

Intercalated composites: In this case, polymer chains intercalate spaces between platelets [25]. Although intercalated chains bring about expansion between the silicate layers, these stacks of layers are still preserved.

Mixed intercalated and exfoliated nanocomposite: Conceptually, exfoliated and intercalated clays are partially present in this type of nanocomposites. Exfoliation is achieved in some extend besides intercalation which is also pronounced for the same system (Figure 4).

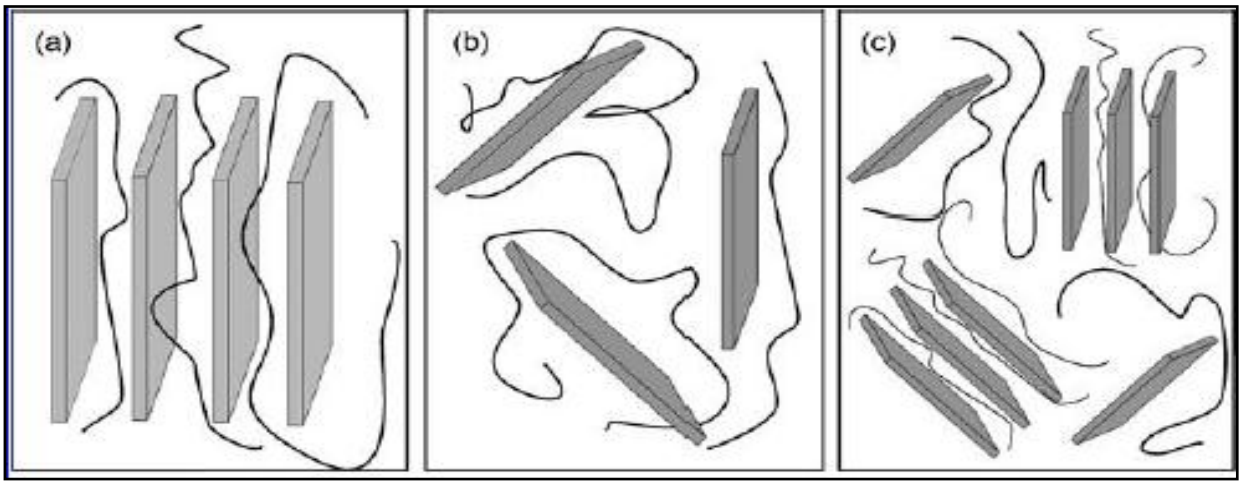

Figure 4: Schematic representation of the various PLSN architectures: (a) Intercalated, (b) Exfoliated, and (c) Mixed intercalated–exfoliated [26].

1. 2. 4. Preparation Methods of Nanocomposites

Since preparation concept is crucial for nanocomposite fabrication, there are certain ways leading to that. Intercalation of polymers in LSs that act as a host place has been verified to be successful method for producing PLSNs [18]. The preparation approaches of PLSNs can be divided into three main groups regarding the dispersion of the clay in polymer matrix. Most common techniques for formation of PLSNs are in-situ polymerization, solution intercalation and melt blending [27]. In this study it is focused on melt blending technique.

1. 2. 4. 1. Melt Blending Method

Melt intercalation method has great advantages compared to in-situ intercalative polymerization and solution intercalative polymerization. Firstly, the absence of organic solvents during processing makes this method environmentally sound. Secondly, it is favorable to use current industrial mixing and processing techniques [18]. Since direct melt intercalation is highly specific for the polymer, it offers new polymer clay hybrid systems that were previously not suitable by in-situ or solution polymerization methods [15]. Regarding the advantages of this method there has been some studies performed by that (Figure 5).

First leading research was done by Vaia, Ishii and Giannellis [28] via melt intercalation.They investigated formation of PS clay nanocomposite and its thermal stability by melt blending method. In the work of the group they described a new process for direct polymer intercalation based on enthalpic mechanism. By maximization of the number of polymer host interactions unfavorable loss of conformational entropy associated with intercalation of the polymer can be overcome leading to new intercalated nanostructures. They used derivative of MMT mica-type layered silicate (MTS) as a host. MTS was treated with modifier

dioctadecyldimethylammonium bromide by cation exchange reaction. This modification render hyrophilic nature of MTS gallery organophilic. They demonstrated that for the resulting PS mica-type silicate nanocomposite by this technique had improved the glass transition temperature in the range 50-150^{o}C since interactions between polymer and silicate host markedly increased. This increase attributed to confined rotational and translational motion of intercalated polymer chains between the layers which is analogous to chemical cross links in bulk polymers.

Su, Jiang and Wilkie [24] published a report based on preparation of PS, high impact polystyrene (HIPS) and acrylonitrile-butadiene-styrene (ABS) terpolymer nanocomposites by melt blending. In the study they have made two organically-modified clays, which are copolymer of PS and copolymer of methyl methacrylate (MA) modified clays to produce nanocomposites. They observed that in some cases exfoliated nanocomposites were found. Better exfoliation was achieved by organic modification of the clays made of copolymers of PS. This manipulation in the clays tackled the problem of intercalation of aformentioned polymer chains within the galleries by increasing the chance of compatibility. Exfoliation was also proven by X-ray diffraction (XRD) patterns from the nanocomposites formed PS modified clays while mostly tactoids were present for polymer MA modified clay composites. XRD results were complemented with TEM images to verify complete exfoliations in the systems and TEM results were complied with XRD patterns. Thermal stability test results of the nanocomposites showed that thermal degradation started at high temperatures for PS modified clay nanocomposites when compared with MA modifed clay microcomposite. However regardless of dispersion of clays it was seen that no differences were detected in heat release reduction between nanocomposite and microcomposite. The same was pronounced for mechanical testing results unless further increase in amount of clay was made in the composite systems.

Figure 5: Schematic depicting of the melt intercalation process between polymer chain and organo modified clay [29].

1. 2. 5. Characterization Methods of Nanocomposites

Generally, the work with optimization and development in the structure of nanocomposites is followed with a number of methods in order to determine degree of exfoliation and compare it to other samples. These methods have been clarified in the literature for this purpose. WAXD analysis and TEM are essential two methods [7]. Due to its easiness and availability WAXD is the most common technique to characterize nanocomposite structure. Nanocomposites containing intercalated silicate particles that result in higher *d-spacing* give new basal reflections which correspond to larger gallery height [15]. WAXD can introduce a convenient method to obtain the *d-spacing* of the silicate layers and intercalated nanocomposites but little

information can be deduced about the spatial distribution of the silicate layers. In addition to this, since some layered silicates do not exhibit well-defined basal reflections, broadening in peaks and decrease in intensity becomes more difficult to study. Hence interpretations based on WAXD diffractograms are ambiguous. To offset the deficiencies of WAXD, TEM images can be utilized. One can get understanding of internal structure, spatial distribution of different phases and views of the defect structure throughout TEM images. Both TEM and WAXD are considered fundamental tools to evaluate nanocomposite structure [30]. However, TEM is time consuming method and supply qualitative information on a certain region of the sample while WAXD provides quantitative information on basal spacing changes in the silicate layers. In addition, sometimes small angle X-ray scattering (SAXS) can also be used for characterization of the nanocomposites' structure. SAXS becomes useful when the layers are disordered in exfoliated nanocomposites or intercalated nanocomposites whose basal spacing exceeds 6-7 nm [7].

Although WAXD and TEM are well-known devices for the characterization of composites, there are other techniques allowing further analysis on nanocomposites. In this study some of these techniques were used and described briefly as follows in accordance with the purpose of this work.

TGA (Thermo-Gravimetric Analysis) is a tool to characterize PLSNs. On one hand, TGA can be used to investigate intercalation degree of modified clays in terms of percentage of organic surfactant on the other hand TGA is used to quantify thermal stability of PLSNs. Onset of degradation is recorded commonly in order to identify the improvement in PLSN when compared with original polymer [31].

DSC (Differential Scanning Calorimetry) is based on measuring heat flow that occurs in a sample when it is subjected to heating, cooling or holding isothermally at constant temperature. DSC technique allows to detect endothermic and exothermic effects and determine specific heat capacity of the sample. For instance, this method is useful to determine physical transitions such as T_g of amorphous materials, melting point, crystallization behavior, and chemical reactions thermal decomposition, depolymerization, polymerization, oxidative decomposition and so on [32].

Instead of TEM, HR-SEM (High Resolution Scanning Electro-Micrograph) can be used for sake of morphological investigation of composites. This equipment ensures observation and characterization of heterogeneous organic and inorganic materials on nanometer (nm) to micrometer (μm) scale. It is substantial device owing to capability of obtaining three-dimensional images of the surfaces of a very wide range of materials. It also enables to provide both qualitative and quantitative elemental information from the area of a sample 1 μm in diameter and 1μm in depth hence internal structure and spatial distribution of different phases can be ensured by SEM. One can take topographic images of a sample in magnification range 10-10000X with the SEM [33].

UV/VIS spectroscopy can be used to determine optical clarity of the resulting composites. Since one of the essential and useful aspect of nanomaterials is their optical properties, these

properties of nanomaterials depend on parameters such as feature size, shape, surface characteristics, and other variables including doping and interaction with the surrounding environment or other nanostructures [34]. In particular, the size of the particles used for nanocomposite preparation plays a key role for observing transparency in a material. Thus, the transparency of a nanocomposite film depends on the size of the particles used. An introduction of a material with a refractive index (RI) n_p, different from that of the matrix n_m, leads inevitably to light scattering and results in opaqueness. However, the RI mismatch can be compensated by decreasing particle size below the wavelength of visible light. Generally, studies have shown that, depending on the degree of RI mismatch, an intensity loss through scattering becomes negligible if the particle size is below 100 nm [35].

Improvements in gas barrier property can be obtained through incorporation of clay nano-particles depending on the clay distribution and orientation. Measurement of the gas permeation through the polymer composites can be made using many different direct and indirect methods. One of the common methods for the permeation measurements is measuring the permeability directly as composite property in the commercial gas transmission rate measuring equipments. The oxygen transmission rate through nanocomposite films and laminates can be measured at different temperatures as well as different relative humidities. The test requires samples in the form of a film or foil [6].

1. 2. 6. Nanocomposite Properties

1. 2. 6. 1. Mechanical Properties

1. 2. 6. 1. 1. Tensile Properties

Polymeric nanocomposites prepared with layered silicates has shown remarkable improved tensile modulus. Most of the studies reveal the tensile properties as a function of clay content. N6 nanocomposite synthesized with in-situ interecalative ring opening polymerization of 1-caprolactam resulting in formation of delaminated nanocomposite demonstrate notable increase in tensile properties at low content of filler. The main reason for this enhancement can be considered strong interaction between clay surface and polymer matrix via formation of hydrogen bonds (Figure 6). In nanocomposites, improvements in tensile properties depend on average length of the clay particle thus the aspect ratio. In Figure 7 correlation between tensile modulus E and exfoliated N6 nanocomposites with various clay content at 120^{o}C is shown in [15].

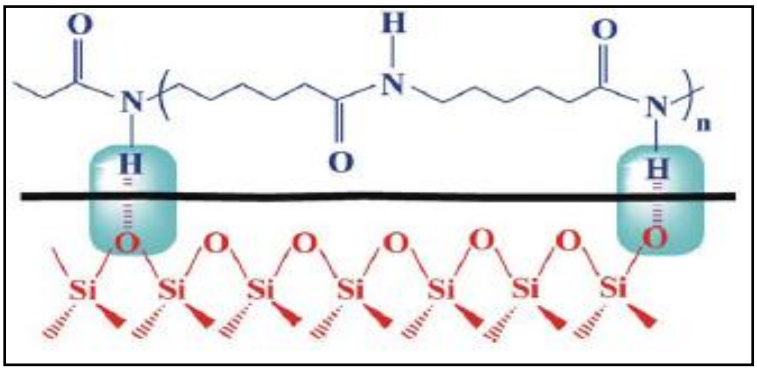

Figure 6: Schematic illustration of formation of hydrogenbonds in N6/MMT nanocomposite by in situ polymerization [15].

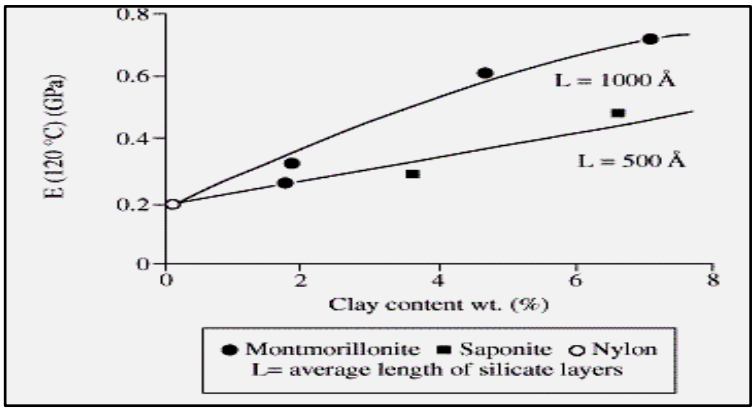

Figure 7: Effect of clay content on tensile modulus in N6/OMMT nanocomposite prepared by melt intercalation [36].

1. 2. 6. 2. Thermal Stability

TGA is frequently use to analyze thermal stability of a polymeric material. The weight loss is monitored as a function of temperature after formation of volatile materials at high temperatures. When TGA is carried out under an inert gas flow such as Nitrogen (N_2), Helium (He) or Argon (Ar) this type of heating is called a non-oxidative degradation contrary to oxidative degradation where O_2 gas is used for heating the samples. Generally, presence of the clay in the polymer matrix is considered to improve the thermal stability by acting as a superior insulator and mass transport barrier to the volatile products released during degradation [15].

Blumstein reported on improvement of thermal property of poly(methyl methacrylate) (PMMA) LS nanocomposite. In his work, preparation of nanocomposite was based on free radical polymerization of MMA inside the galleries of clay. He found that PMMA clay nanocomposite was thermally stable at higher temperatures at which neat PMMA is anticipated to completely degrade. TGA result showed that PMMA clay nanocomposite had 40-50^{o}C higher decomposition temperature. Blumstein attributed that increment to restricted thermal motion of PMMA in the gallery [37].

1. 2. 6. 3. Flame Retarding Properties

The flame retardancy of polymers is substantially important in many applications. In past years brominated flame retardants dominated additives used in polymers. Studies showed that clay nanocomposites were revealed to decrease remarkably level of flame retardancy. In the case clays appear to help nanocomposite to form char and this char acts as an insulative layer to slow down heat transfer and retard movement of gases to feed the flame [2]. The cone calorimeter is one of the most effective methods to study flame retardancy of polymeric materials. Properties, associated with flame retardancy, such as heat release rate (HRR), peak HRR, smoke production, and carbon dioxide (CO_2) yield are essential to evaluate the fire safety of materials [15]. Gillman et al. [38] reported studies with cone calorimetry showing that enhancements in flame retardancy property in polymers such as PP, PS, N6 was achieved in the presence of clay. This was characterized by formation of char which was developed on the outer surface during combustion. This char on the surface acts as insulator barrier for O_2 as well as combustion products generated during decomposition to prevent further burning.

1. 2. 6. 4. Gas Barrier Properties

In PLSNs clays are considered to enhance the barrier properties by creating maze or tortuous path that restricts the progress of the gas molecules through the matrix resin [15]. Nielsen proposed simple model to describe the effect of clays on permeability in filled polymers. This model is based on tortuous path created by layered silicates. Presence of clay introduces longer pathways in the matrix for diffusing gases thus reduces the permeability (Figure 9). In particular, as it can be seen in Figure 8 a sheet-like morphology is efficient in creation tortuous paths in polymer matrix owing to high aspect ratio when compared to other types of filler such as cubic, spherical shaped [13]. Lan et al. [39] reported that in polyimide nanocomposite relative permeability fit tortuous path model for O_2, CO_2, water vapor (H_2O) and ethylacetate vapors. They showed that permeation of polyimide nanocomposite was reduced ten times higher with synthetic mica at 2 wt.% clay loading than that of pure polyimide.

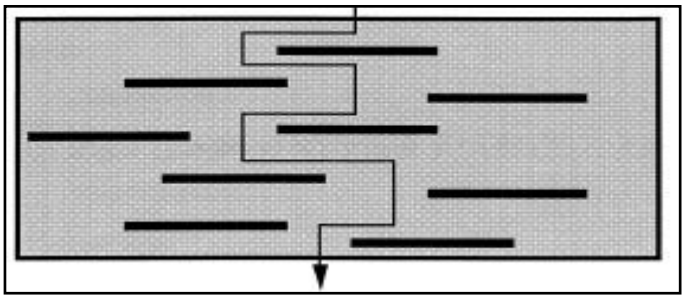

Figure 8: Proposed tortuous pathway model for diffusive gases in the presence of sheet-like clays with high aspect ratio [22].

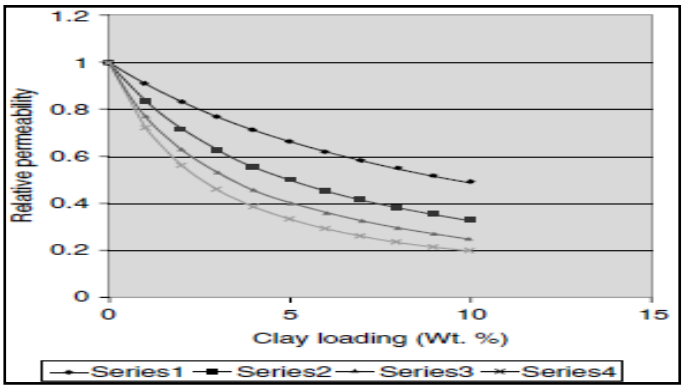

Figure 9: Nielsen model; relative permeability vs clay loading in different clay loadings with various aspect ratio 50, 100, 150, 200 referring to series 1 to 4, respectively [2].

1. 2. 6. 5. Optical Clarity

Despite silicate layers are micron size in lateral dimension, they are pronounced around 1 nm in thickness. When the clay exfoliation is accomplished leading to dispersion in the polymer matrix, and the aspect ratio is less than 400 nm, the resulting nanocomposite is optically clear in the visible light. For sake of comparison, UV/VIS transmittance spectra of pure PVA and PVA/Na^+MMT nanocomposite containing 4 wt.% and 10 wt.% are demonstrated in Figure 10. The spectra show that visible region is not affected by the presence of the silicate layers and transparency of PVA is retained. Various nanocomposites prepared with organo modified clays also show optical transparency [39].

s

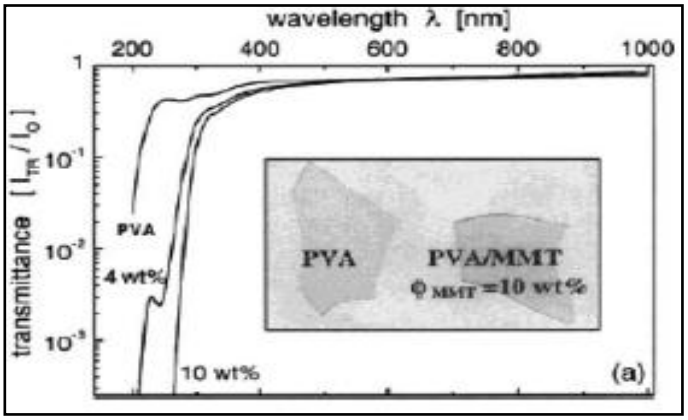

Figure 10: UV/VIS transmittance spectra of PVA and PVA/Na^+MMT nanocomposites containing 4 wt.% and 10 wt.% clay [39].

2. EXPERIMENTAL

In this section starting materials, sample preparation techniques and characterization methods are described for fabrication of PS/MMT nanocomposites.

2. 1. MATERIALS

PS was general purpose polystyrene (GPPS) with the commercial brand name Empera 332N from Ineos Nova Company. Unmodified MMT and three types of modified MMT clays were used as received, kindly supplied by three different companies. Modified Dellite 67G supplied from Laviosa Company (Italy) with aspect ratio 500nm, modified Nanofil SE 3010 and Cloisite 11B clays were supplied from Southern Clay Company (USA) with no specified aspect ratio. Unmodified MMT was acquired from Nanocor Company (USA). Modification type is dimethyl dihydrogenated tallow alkyl ammonium cation for both Dellite 67G and Nanofil SE 3010 while for Cloisite 11B the modification is dimethyl benzyl hydrogenated tallow alkyl ammonium cation where hydrogenated tallow refers to organic content ~65% C18;~30% C16;~5% C14.

2. 2. SAMPLE PREPARATION

2. 2. 1. Preparation of PS/MMT Masterbatches

Three types of PS/MMT masterbatches were produced by melt blending using a co-rotating twin screw extruder Brabender Plasti-Corder with a TSE 20/40 D equipped with a volumetric main and side feeder. Its screw length is 800mm and its L/D ratio is 40. The composition of masterbatches was containing ~20 wt.% MMT and was calculated from the amount of clay and polymer charged to the extruder.

In the beginning of the manufacturing process, the content of clay alone in three different OMMT´s Dellite 67G, Nanofil SE 3010 and Cloisite 11B was determined by TGA. Since the extruder has volumetric main and side feeder, there was a need to calculate gravimetric input to the extruder for the production of required ~20 % masterbatch composites. Temperature in the extruder was set to 180^{o}C for the first temperature zone and remaining five zones was set to 190^{o}C. Screw speed was set to 50 rpm for three modified clays. The reason to use low temperature values was to avoid degradation of both organic modifier in clays and PS during fabrication. Main problem to tackle during production of the masterbacthes was the clogging of the side feeder screws which push clay powder into the extruder in order to obtain ~20 % masterbatch composites. When the side feeder was connected to the extruder during masterbatch production, screws were faced with the heating. It was deduced that clogging occurred due to excess heating in the screws of the side feeder. Therefore, processing temperature caused clay powders to adhere on the screws. That adhesion was attributed to size of the clay powder and organic modifier of the clays. This affected the amount of clay that needs to be pushed into the extruder so that special care was needed to take for the right amount of clay loading. After calculations for the exact amount of the clays and polymer to be charged,

required clay content was obtained for each masterbatches. As it can be seen from Table 2 screw speed, main feeder speed and side feeder speed values were the same for the clays Dellite 67G and Nanofil SE 3010 but the main feeder rate had to be decreased for the clay Cloisite 11B maybe because of the lowest content organic modifier. This was done due to the aforementioned clogging effect of the side feeder screws exposed to high temperature for long time. After formation of masterbatches, cryo-grinding, by cooling the samples in liquid nitrogen, was performed to prepare powder for the production of nanocomposites. Table 2 shows the parameters of the extruder during production of masterbatches.

Table 2: Parameters for extrusion of the masterbatches with modified clays.

Modified MMT Clays	Screw speed (rpm)	Main feeder speed (rpm)	Side feeder speed (rpm)	Content of clay (wt.%)
Dellite 67G	50	10	180	16.7
Nanofil SE 3010	50	10	180	17.4
Cloisite 11B	50	7	180	20.2

2. 2. 2. Preparation of PS/MMT Nanocomposites

The prepared masterbatches were used for the production of PS/MMT composites containing the final proportion (4-5 wt.%) clay. The same method was implemented, as it has been done for formulating the PS/clay masterbatches. Melt blending processing was applied and temperatures were set to the same values 180-190^{o}C starting from the first heating zone to the sixth one. Clay proportion of composites was calculated from the amount of masterbatch and polymer introduced to the extruder.

For the formation of nanocomposites two different screw speeds were selected viz. 150 and 75 rpm referring to high loading of polymer in different speeds. The goal was to obtain high shear forces in order to facilitate delamination of clay particles and disperse them successfully in the PS matrix thus resulting in nanocomposites. Increased shear forces were indicated by increased torque values. Then calculated amount of masterbatches was loaded to extruder from the side feeder. In this case the problem of clogging did not arise during production of composites when the side feeder was attached to the extruder. This might have been due to particulate size of grinded masterbatches, which was much bigger compared with the size of the modified clays' powder. Composites were acquired from ribbon type of die in the form of film in width 5-7cm and thickness 200-350μm. In Table 3 parameters for manufacturing of composites are demonstrated below. The resulting composites were prepared in hot pressing machine with demanded thickness for further characterization. Preparation method of composites in hot pressing machine is based on method reported by S. Nazarenko et al. [11].

Pieces of composites were loaded on a metal plate covered with aluminum foil with cavity thick spacer about 200μm. The plate was placed in a preheated press at 190^{o}C and held for 10 min without pressure and then a pressure of 7.35 MPa was applied and released. This cycle was repeated three times to have aimed plaques free of air bubbles. Finally the pressure was applied

for 5 min and then released. Formed plaques were allowed to cool down. Then these plaques were used to conduct various measurements.

Table 3: Parameters for nanocomposites fabrication during extrusion.

Masterbatch	Screw speed (rpm)	Main feeder speed (rpm)	Side feeder speed (rpm)	Torque (N.m)	Content of clay (wt.%)
PS/Dellite 67G	150/75	50/25	74/38	50/45	4.1
PS/NanofilSE3010	150/75	50/25	178/93	48/40	4.2
PS/Cloisite 11B	150/75	50/25	98/52	51/46	4.9

2. 3. CHARACTERIZATION TECHNIQUES

2. 3. 1. WAXD

WAXD was utilized for characterization of basal spacing of the clays in PS/ clay masterbatch composites and organo modified clay samples. WAXD diffractograms were recorded in 2 theta scale 2° to 10° by increments 0.02° in 4 sec. step time with a Siemens D 5000 (Germany) diffractometer operating with a source CuK_α λ = 1.5406Å and generation tension was 40 kV, generator current was 25 mA.

2. 3. 2. TGA

TGA was performed using a TGA/DSC 1 instrument (Mettler Toledo, USA) equipped with a gas controller (GC 200). The tests were performed by applying a temperature programme containing a dynamic (10^oC/min) part from 25^oC up to 570^oC in inert atmosphere (N_2, 50 ml/min) followed by a 30 min isothermal oxidative environment (O_2, 50 ml/min). Organo modified MMT samples and PS/OMMT composites were used to determine clay contents and improvement in thermal stability of resulting composites.

2. 3. 3. DSC

DSC was conducted under inert, N_2 flow, 50 ml/min using DSC 1 (Mettler Toledo) instrument equipped with a (GC 100) gas controller. Method was set up in two steps starting at temperature 25^oC for 3 min isothermally and increased to 140^oC at a heating rate 20^oC/min around 6 min then at 140^oC isothermal part was applied for 2 min and the first step was completed by decreasing temperature from 140 to 40^oC with the same cooling rate 20^oC/min for 5 min. Second step was started at temperature 40^oC for 4 min and increased to 150^oC in 5 min heating rate was the same for the second step as it was in the first cycle.

2. 3. 4. MECHANICAL TESTING

Tensile testing measurements for dumbbell shaped samples was carried out using Zwick Z100 (Germany) instrument equipped with a 2.5 kN load cell and a video extentiometer. The tests were performed in a standard climate (23±2°C, 50±5% RH) on dumbbell shaped specimens using a test speed 1 mm/min and a preload of 1 N. The test specimens were prepared using SS 162202 type of puncher in dumbbell shape.

2. 3. 5. HR-SEM

Zeiss Supra 40 VP (Germany) HR-SEM was employed for taking images of resulting composites. Depending on the need to have different levels of charged sample surface for aiming high resolution, HR-SEM was operated between 0.7-1.5 kV acceleration voltage. Samples were analyzed directly as well as after gold sputtering. The sputtering was performed on fractured surface by using an Agar Coater Sputter Model 109 (England) device under 0.08 mbar pressure and 35 mA generator current for 35 sec.

2. 3. 6. UV-VIS

UV-VIS spectroscopy was performed to obtain transparency property of resulting composites. Wavelength range was selected 200-800nm using Perkin Elmer Lambda 19 UV/VIS/NIR Spectrophotometer (USA) equipped with Deuterium lamp radiated from $2cm^2$ window for transmittance measurement. Two measurements were performed for each material. The thickness varied between the samples (325-450µm) and the results were therefore recalculated based on a common thickness of 300µm.

2. 3. 7. GAS PERMEATION

Gas barrier measurements for O_2 gas were conducted at 23^oC using YSSY AG L 100-5000 Manometric Gas Permeability Tester (Switzerland). Duplicate measurements were performed for each composite having thickness in the range 295-420µm.

3. RESULTS AND DISCUSSION

3. 1. WAXD RESULTS OF THE MODIFIED CLAYS AND THE MASTERBATCHES

WAXD pattern is presented in Figure 11 for three organo modified clays. It should be noted that particularly there are different levels of intercalation for Dellite 67G and Nanofil SE 3010 so that three diffraction orders were detected for Dellite 67G and Nanofil SE 3010 identified with three identical peaks. These peaks were interpreted by Braggs law. According to Braggs law $n\lambda=2d\sin\theta$ [40] interlayer distance 'd' is reciprocally proportional to angle 'θ'. Then when *d-spacing* increases diffraction peaks will appear at lower angles while peaks at higher angles indicate small interlayer distances. In Figure 11 first order peak for Dellite 67G observed at small angle is 2.49° referring to the largest distance between clay layers d_{001}= 35.28Å and indicating a considerable intercalation. In the second order peak the distance detected was at relatively higher angle 4.77° with corresponding *d-spacing* d_{002}= 18.5Å showing that some degree of modification has been achieved. Last peak in the diffractogram refers to no intercalation and was achieved at all indicating *d-spacing* d_{003}= 12.17Å with corresponding angle 7.26°. In addition, considering the area under the peaks it can be deduced that amount of intercalation varies for the clays. Intensity of the peaks can be assessed for estimating the amount of intercalation in the clays. In this respect, it can be said that for the first order spacing, the highest intensity is present hence most of the intercalation type is pronounced for the first order spacing. The proportion of clays with second and third order spacing is quite small.

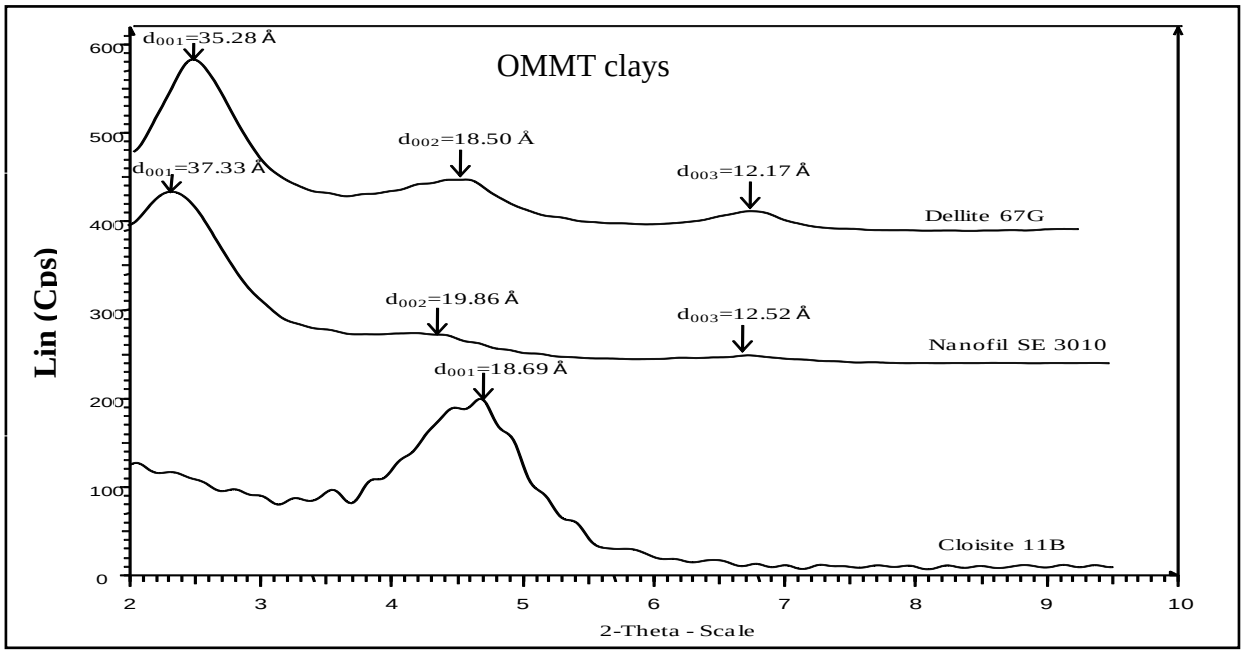

Figure 11: WAXD diffractogram of clays.

Similarly, for Nanofil SE 3010 three different peaks were detected. When the Braggs law is applied to the WAXD pattern from Nanofil SE 3010, the interlayer distance d_{001}= 37.33Å with higher amount of intercalation can be seen with corresponding angle 2.37°. The second and third order *d-spacing* d_{002}= 19.86Å, d_{003}= 12.52Å were detected with corresponding angles 4.45° and 7.06° respectively. Nevertheless, for Cloisite 11B, *d-spacing* was obtained with maximum

interlayer distance d_{001}= 18.69Å at angle 4.72° by a single peak detection. WAXD patterns for each clay are tabulated below in Table 4.

Table 4: WAXD diffractograms for OMMTs.

OMMT	***d-spacing* (Å)**			**Corresponding angle 2θ**		
PS/Dellite 67G	35.28	18.50	12.17	2.49°	4.77°	7.26°
PS/Nanofil SE 3010	37.33	19.86	12.52	2.37°	4.45°	7.06°
PS/Cloisite 11B	18.69			4.72°		

WAXD diffractograms were also obtained for the PS/MMT masterbatch composites while PS/MMT final composite samples containing low clay content gave weak X-ray patterns. WAXD patterns for the masterbatch composites are shown in Figure 12. The results were comparable enough with the modified MMTs and but had surprisingly appeared at higher angle values. At first glance, from the patterns one may deduce that no intercalation of the polymer chains inside the clay galleries took place. However, this inference might be misleading. Appeared diffracted peaks could be interpreted as newly formation of interlayer distances due to intercalation of PS chains inside the clay galleries in PS/Dellite 67G and PS/Nanofil SE 3010 masterbatch composites while diffracted peaks showed that interlayer distance was remained the same for PS/Cloisite 11B masterbatch composite. Formation of new peaks in Figure 12 and disappearance of previous peaks in Figure 11 could be assessed as indication of some intercalation of modified clays for PS/Dellite 67G and PS/Nanofil SE 3010 masterbatch composites. Besides, in PS/Closite 11B masterbatch composite some changes in *d-spacing* were also detected. Particularly, these changes can be recognized easily at the onset of diffraction at very low angles (2-3°) referring to remarkable increase in interlayer distance (30-40Å) when compared to OMMT diffractogram. Diffraction results are shown in Table 5 for the masterbatch composites.

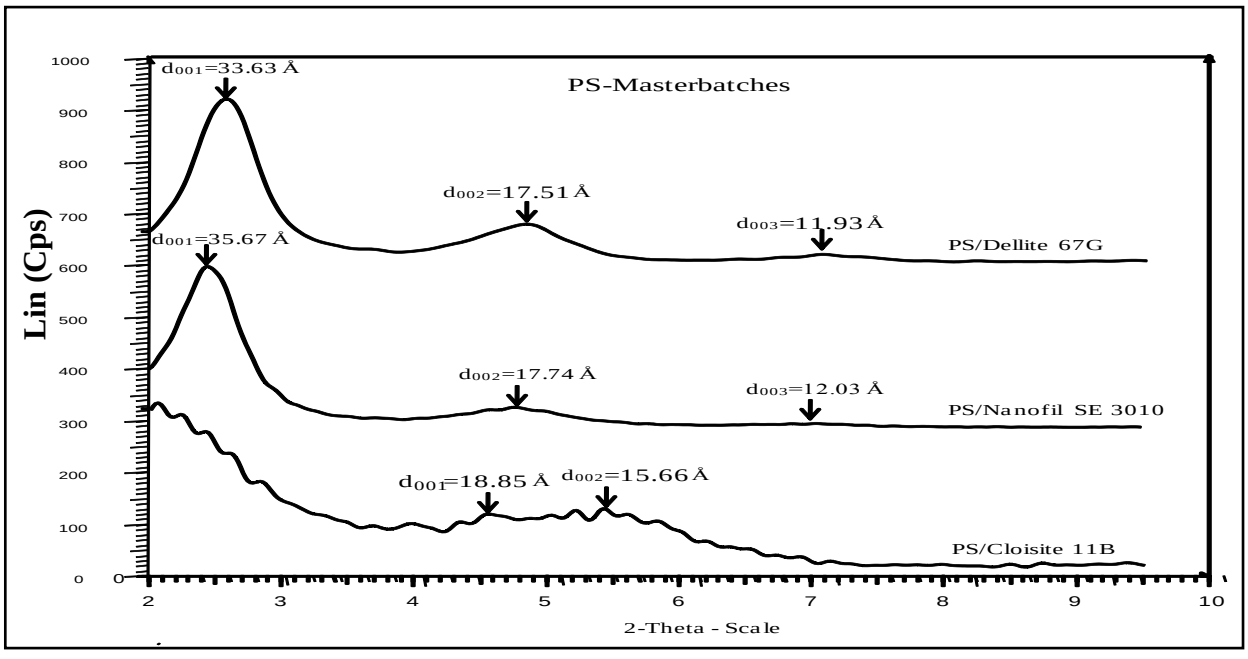

Figure 12: WAXD patterns for masterbatch composites.

Table 5: WAXD results of PS/MMT masterbatches.

Masterbatch	*d-spacing* (Å)			Corresponding angle 2θ		
PS/Dellite 67G	33.63	17.51	11.93	2.62°	5.04°	7.40°
PS/Nanofil SE 3010	35.67	17.74	12.03	2.47°	4.98°	7.34°
PS/Cloisite 11B	30-40	18.85	15.66	2-3°	4.68°	5.64°

3. 2. HR-SEM IMAGES

Morphology of the resulting microcomposites was monitored using HR-SEM. Figure 13 shows images of the PS/Dellite 67G and PS/Nanofil SE 3010 composites. HR-SEM provides direct proof of formation of delaminated microcomposites for both PS/MMT blends. Relatively good dispersion of clay particles, which are stacked from tens up to hundreds of nanometers in thickness, was achieved successfully. However, incompatibility (dark sections around the clay particles pointed out with arrows) of these clay particles with PS matrix can be easily recognized from the pictures.

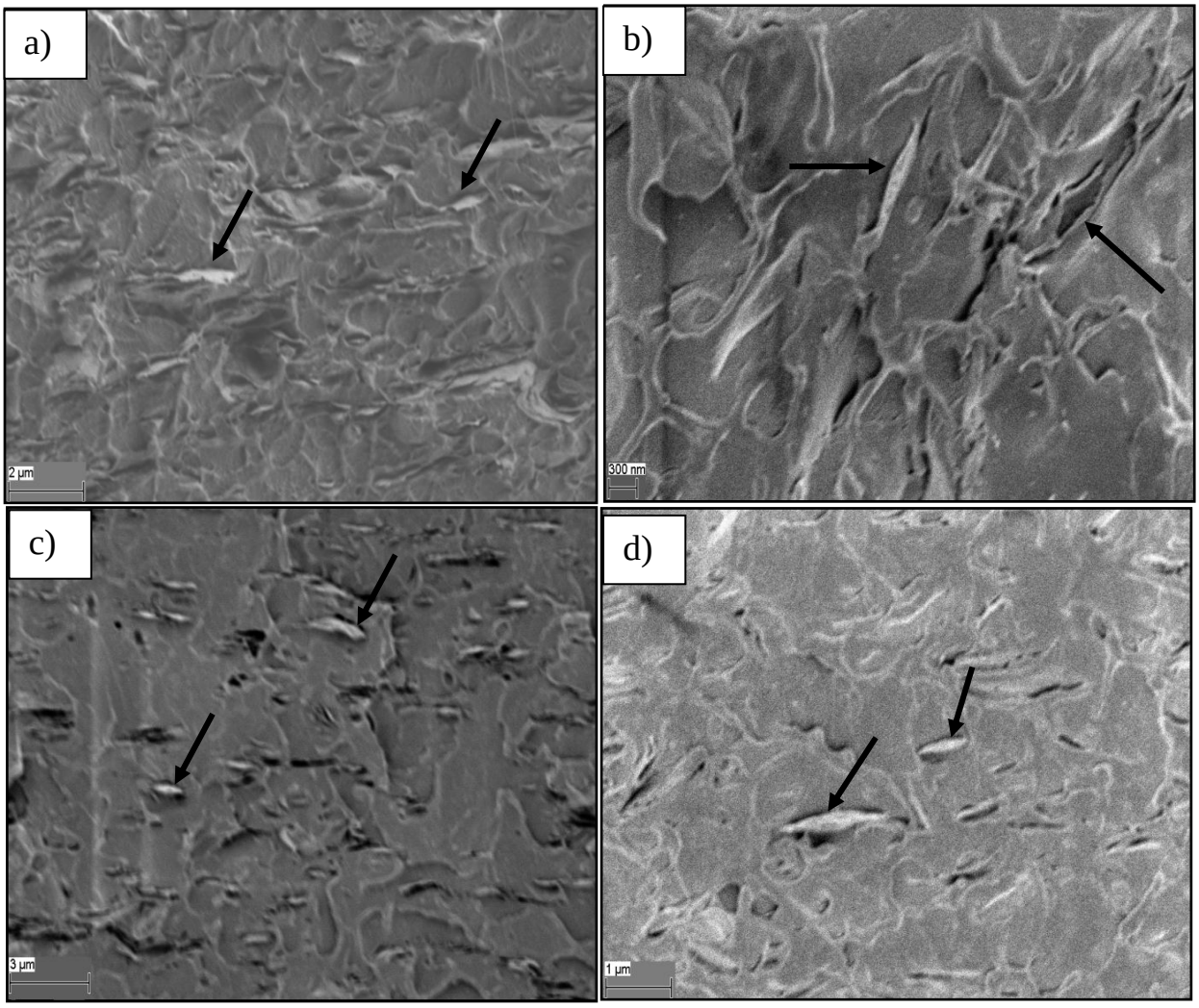

Figure 13: HR-SEM images of (a-b) PS/Dellite 67G and (c-d) PS/Nanofil SE 3010 composites.

In Figures 14 and 15 images for the PS/Cloisite 11 B composite are shown under different magnification. For PS/Cloisite 11B two separate phases was observed in Figure 14 where clay particles covered by the PS matrix resulting in formation of heterogeneous structures in the material. In this type of microcomposite, the size of clay particles is relatively bigger than this of the former microcomposites. No pronounced delamination of clay particles can be detected for this type. Poor compatibility is also present in the blend analogous to the former ones as expected.

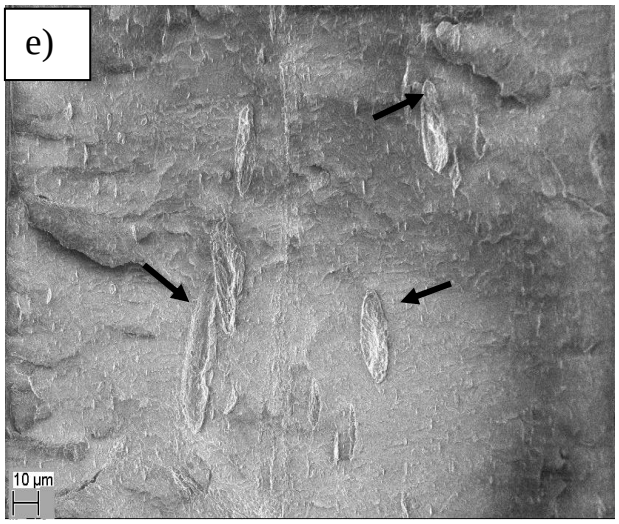

Figure 14: Heterogenous two phases structure comprising of clay particles and PS matrix in micron size for PS/Cloisite 11B microcomposite (e).

As a result of HR-SEM images, preparation of these three types of composites led to formation of either delaminated/intercalated (a, b, c, d) or mixed (e, f, g) microcomposites by the melt blending method.

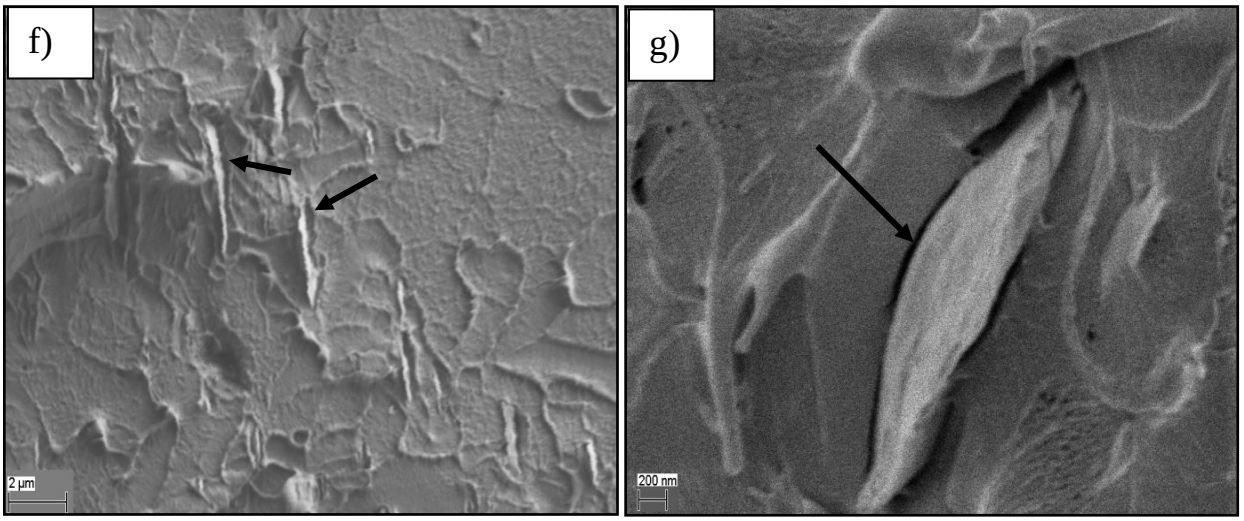

Figure 15: HR-SEM images of PS/Cloisite 11 B composite at higher magnification (f-g).

3. 3. TGA OF THE CLAYS AND COMPOSITES

TGA analysis was performed for determining organic modifier content of the clay samples used in composites and pristine MMT. Amount of modifier contents are tabulated in Table 6 for three clays. Although there is no modification on pristine MMT, the reason to perform TGA measurement was to have reference curve for calculating exact amount of organic modifier intercalated between the clay platelets thus obtaining correct composition of final microcomposites. In particular, measurements have been done under N_2 flow to avoid oxidation, which might have caused miscalculations in modifier content. Onset temperature was 25^{o}C and was increased up to 570^{o}C over which crystal structure of the clay is changed leading to some mass loss. In order to determine the organic carbon residue the test programme was complemented with thermo-oxidation process to obtain only residual amount of clay from organo modified ones.

When one has a closer look at the TGA curve for pristine MMT in Figure 16 two distinct steps can be seen to be considered. At the onset of the TGA curve in step I, drastic mass loss was detected until 90^{o}C. This mass loss was attributed to the loss of moisture that was already present in the galleries of the pristine clay. Furthermore, at the temperature range between 470^{o}C and 570^{o}C (step III) another mass loss was taken place. The mass loss observed in this step was considered as decomposition of the clay's crystal structure.

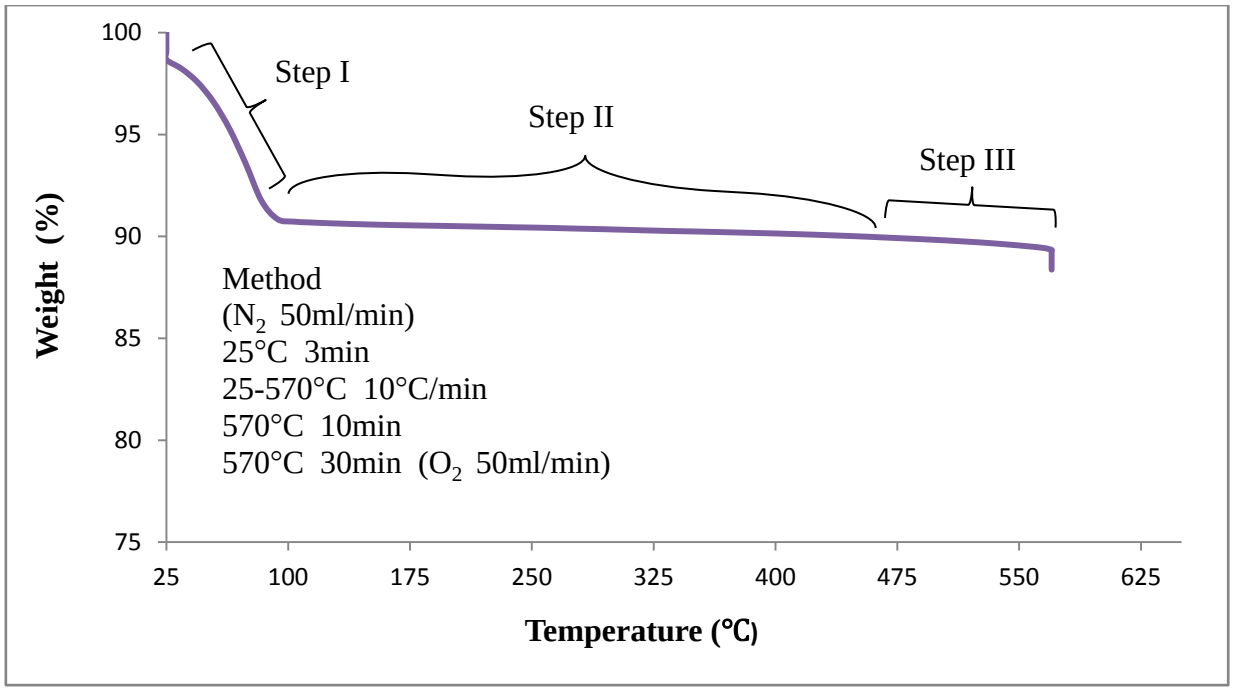

Figure 16: Decomposition of pristine MMT.

The real modifier content of organo modified clays was assessed by eliminating steps I, III from step II. In this respect, TGA curves of the second step, which starts from temperature 90^{o}C until 470^{o}C, were considered that it is the mass loss due to thermal degradation of intercalated

organic modifier of the clay samples only. TGA curves of the modified clays are illustrated in Figure 17 and the amount of modifier and clay content are tabulated in Table 6.

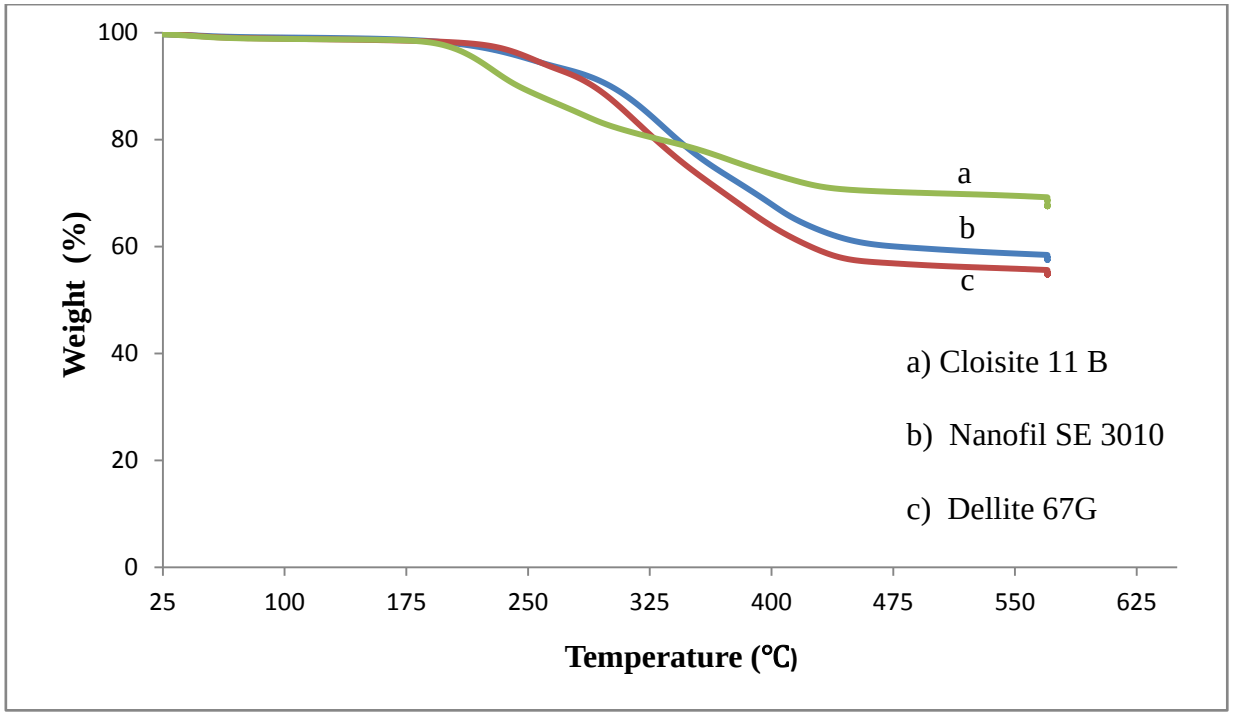

Figure 17: TGA curves for modified clays Dellite 67G, Nanofil SE 3010 and Cloisite 11B.

Table 6: Amount of modifier and residue for each clay.

Modified Clay	Organic Content (wt.%)	Clay Residue (wt.%)
Dellite 67G	43.6	56.4
Nanofil SE 3010	42.0	58.0
Cloisite 11B	30.5	69.5

The same calculation method, which has been described above for obtaining amount of modifier content, was applied when identifying the clay content of the final composite materials. In this case step I did not appear due to vaporization of moisture during processing. Figure 18 and Table 7 show thermal behavior and composition of the final composite materials.

In assessing improvement of thermal stability, composites prepared with PS/Dellite 67G, PS/Nanofil SE 3010 and PS/Cloisite 11B degraded at around 437^{o}C while pristine PS degraded at around 417^{o}C. This shows that resulting composites start to decompose at an about 20^{o}C higher temperature compared to virgin PS. This reveals that partial delamination of the clays was achieved leading to increase in thermal stability. In Figure 18 this increase in temperature was indicated for the three microcomposites. Surprisingly, even though no significant delamination occurred for the PS/Cloisite 11B microcomposite, its decomposition behavior is very likely similar to the delaminated ones. This shows that delamination/intercalation did not make any remarkable change in thermal decomposition property of the former microcomposites when compared with PS/Cloisite 11B microcomposite.

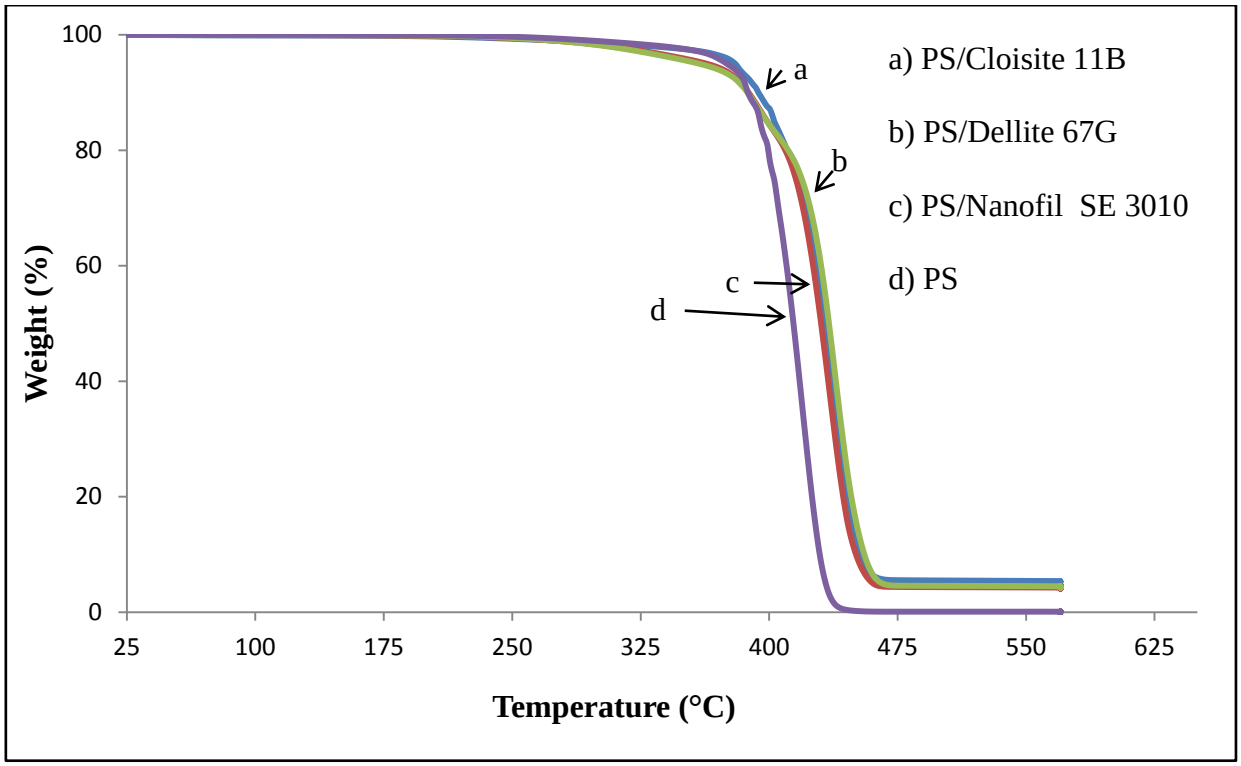

Figure 18: Comparison of thermal stability of PS/MMT composites and pure PS in TGA.

Table 7: Amount of organic content and clay residue in the final composite materials.

Amount of clay in final composite material	Clay Residue (wt.%)	Organic Content (wt.%)
PS/Dellite 67G	4.1	95.9
PS/Nanofil SE 3010	4.2	95.8
PS/Cloisite 11B	4.9	95.1

3. 4. DSC ANALYSIS OF THE COMPOSITES

DSC results were collected in two cycles. In the first heating step, thermal history of the materials was erased before the second heating step where the T_g of the samples was determined. Generally, addition of clay to a polymer affects thermal properties such as T_g and melting point. One may expect increase in T_g depending on the degree of delamination/exfoliation of the clay particles in resulting composites. Some studies have shown either slight or large increases in T_g while other studies have recorded no increase [12]. Chen et al. [41] reported decrease in formation of PEO/clay nanocomposites. In our study, T_g values were obtained as indicated in Figure 19 and Table 8. The T_g values recorded from the DSC traces for the PS, PS/Dellite 67G, PS/Nanofil SE 3010 and PS/Cloisite 11B were 92.8, 94.6, 94.5 and 90.8^{o}C respectively. As it can be seen there are minor increases and decrease in T_g values for the microcomposites compared to virgin PS. These small increases in former microcomposites were considered as partially confinement of polymer chains intercalated within the galleries of modified clays. That restricts segmental movement of polymer chains thus resulting in decrease in thermal mobility. For PS/Cloisite 11B microcomposite a slight

decrease in T_g can be interpreted that organic modifier has opposite effect in the system and acts as plasticizer, which facilitates the movement of polymer chains, in this type of microcomposite. Modifier could migrate from the clay galleries to the PS matrix and interact with it resulting in decrease in T_g value.

Table 8: T_g values for the neat PS and PS/MMT composites.

Sample	T_g (℃)
PS	92.8
PS/Dellite 67G	94.6
PS/Nanofil SE 3010	94.5
PS/Cloisite 11B	90.8

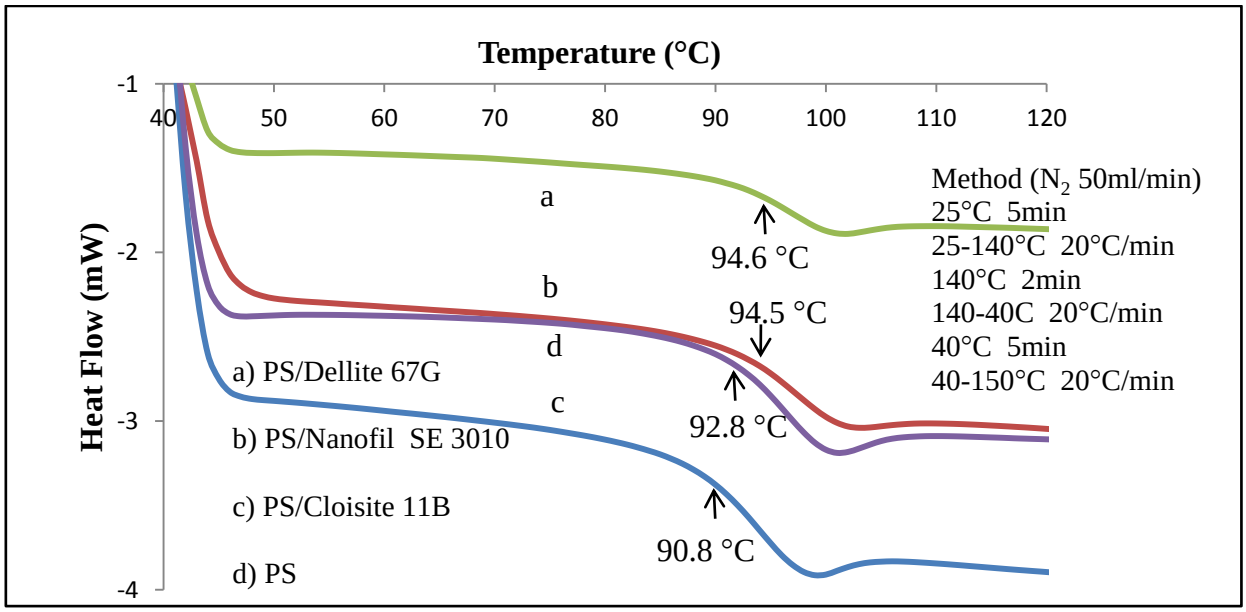

Figure 19: Illustration of DSC traces in determination of T_g for the virgin PS and PS/clay composites.

3. 5. TENSILE TESTING

In general, addition of MMT to a polymer leads to improvement in mechanical properties. Depending on obtaining exfoliated/intercalated and compatible morphology in polymer matrix this improvement is more pronounced. Tensile testing was carried out on dumbbell shaped test specimens for each composite material and pure PS. The presented test results are average values obtained on various number of samples and are tabulated in Table 9.

Table 9: Mechanical properties of PS/MMT microcomposites and PS.

Mechanical properties / Samples	Elongation at break (%) ISO 527-3	Tensile strength at break (MPa) ISO 527-3	E-Modulus (MPa) ISO 527-3
PS	1.20 ($3.3x10^{-3}$, n=4)	32.7 (2.21, n= 4)	2903 (58.2, n=4)
PS/Dellite 67G	-	-	2882 (197.2, n=8)
PS/Nanofil SE 3010	1.00 ($1.55x10^{-2}$, n=5)	29.6 (2.22, n=5)	2909 (55.1, n=5)
PS/Cloisite 11B	1.02 ($0.91x10^{-2}$, n=6)	28.1 (1.39, n=6)	2954 (70.5, n=6)

As it can be seen from Table 9, the Young's modulus is unchanged when compared to neat PS. A slight decrease in elongation and tensile strength at break was found about 16.7% and 9.5% respectively for PS/Nanofil SE 3010 while these data was not monitored for PS/Dellite 67G due to the specimen that fractured outside of the measured section. In evaluation of PS/Cloisite 11B microcomposite a decrease in elongation and tensile strength at break was found viz. 15.0% and 14.1% respectively in comparison with unfilled PS. Generally, insignificant changes were observed in the Young's modulus for the three types of resulting microcomposites. The decrease in tensile strength and elongation at break is related to the lack of compatibility of the two constituents. These observations suggest that more efforts have to be spent to improve exfoliation and compatibility between MMT and PS.

3. 6. UV/VIS TRANSPARENCY MEASUREMENT

UV/VIS transmittance spectrum is shown for the PS/MMT microcomposites and pure PS in operating wavelength range 200–800nm. In Figure 20 transmittance trend of the materials is demonstrated. As it can be realized from transmittance vs wavelength graph, in the visible region (~400-700nm) PS has the highest transparency around 90.8%. At the onset of 400 towards 300nm in UV region transmittance values decreased to about 80% for the pristine PS. On the other hand, transmittance values for the microcomposites PS/Dellite 67G, PS/Nanofil SE 3010 and PS/Cloisite 11B were detected 82.5%, 80%, 85.5% respectively at the end of the visible region (750nm). The spectra showed small differences in transmittance behaviors between three microcomposites in that region. Gradual decreases in transmittance values were observed when the wavelength of the incoming light decreased. Moreover, the diameter of clay particles that is smaller than the wavelength of the visible spectrum results in the incoming light not to be absorbed or scattered by the particles [6]. At 500nm, the transmittance decreased by 11.8% and 15% for the microcomposites PS/Dellite 67G and PS/Nanofil SE 3010 respectively. These reductions in transmittance were attributed to the particle size of delaminated/intercalated clay particles dispersed in the PS matrix. In addition, owing to higher scattering or absorption at lower wavelengths of incoming light, transmittance in UV region was more reduced by approximately 50% around 354 and 376nm for both PS/Dellite 67G and PS/Nanofil SE 3010 respectively. For conventional PS/Cloisite 11B microcomposite,small decrease in transmittance was observed in visible region due to uneven dispersion of clay particles but 50% decrease in transmittance was detected around 300nm. In Table 10 trends in transmittance values are listed for the samples.

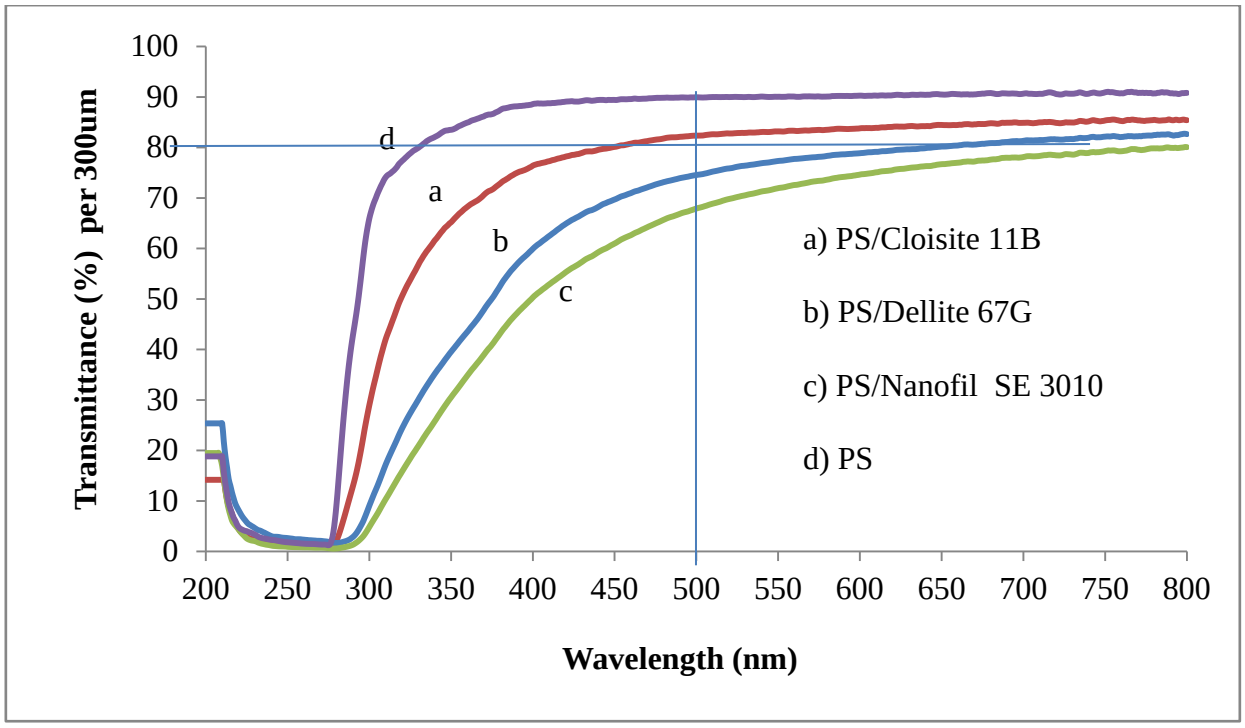

Figure 20: UV/Vis transmittance spectra of PS and PS/clay composites containing 4-5 wt.% clay.

Table 10: Transmittance values in various wavelengths in UV/Vis region for three composites and neat PS.

Sample	Transmittance (%) 300µm thickness			Wavelength (nm)		
PS	90.8	89.9	83.5	800	500	350
PS/Dellite 67G	82.5	72.8	39.5	800	500	350
PS/Nanofil SE 3010	80.0	68.0	30.5	800	500	350
PS/Cloisite 11B	85.5	82.4	65.2	800	500	350

3. 7. GAS PERMEATION OF COMPOSITES

Generally, it is essential to achieve exfoliation and thus individual clay platelets dispersed for increasing gas barrier property in polymeric nanocomposites. That is why the permeability strongly relies on morphology of the nanocomposites. The presence of clay platelets increases the diffusion distance by creating tortuous pathway which the diffusing species must traverse [42]. Permeation tests were performed on plaques from each material (thicknesses 295-420µm). In Table 11 gas permeability trends are shown for the resulting microcomposites in normalized thickness 300µm. As it is pointed out, depending on the exfoliation of the clay, an increase is expected in gas barrier property in the nanocomposites. Considering the fact that in our case for the microcomposites prepared with PS/ Dellite 67G and Nanofil SE 3010 clays, approximately 25% and 27% reduction was obtained in gas permeation respectively. This decrease was attributed to partial delamination and good dispersion of the clay particles comprised of many layers in stacks. However, despite good dispersion and delamination/intercalation lead to

reduction in gas permeability, poor compatibility between two constituents, which possibly creates micro voids around the clay particles, results in an increase in permeation. This also elucidates the reason of small reduction in permeation for PS/Dellite 67G and Nanofil SE 3010 delaminated/intercalated microcomposites. For PS/ Cloisite 11B, this reduction was found about 15% in gas permeability eventhough no delamination/intercalation was achieved and the clay particle size incomparably larger than the former ones.

Table 11: Comparison in O_2 gas permeability of resulting PS/clay microcompsites containing 4-5 wt.% clay residue and neat PS. Normalized to 300µm thickness.

Sample	Gas permeability (OTR**, ml/m^2/day) in 300µm thickness (Index)	Gas permeability (OTR**, ml/m^2/day) in 300µm thickness (ml)
PS*	1.000	531.23
PS/Dellite 67G	0.745	395.51
PS/Nanofil SE 3010	0.732	388.62
PS/Cloisite 11B	0.847	450.08

(*): Neat PS is considered as a reference material (Index= 1.000).
(**): Oxygen gas Transmisson Rate.

Discussion

From the WAXD result of PS/Cloiste 11B masterbatch composite one might have deduced that poor intercalated clay morphology was achieved. Particularly, this indication would be consistent with the HR-SEM images in Figure 15 where the size of clay particles was much larger than that of final PS/Dellite 67G and PS/Nanofil SE 3010 microcomposites. For instance, formation of conventional microcomposite for PS/Cloiste 11B was also revealed from the results of DSC analysis, UV/VIS spectroscopy for transparency and gas permeability measurements. However, DSC result had also surprisingly lower value as not anticipated compared to unfilled PS owing probably to plasticizing effect of the clay modifier. Nevertheless, Increase in thermal decomposition temperature is also observed in this type of microcomposite compared to pure PS.

It is a known fact that when fully exfoliation of the clay is achieved in polymer matrix, significant enhancements in gas barrier and mechanical and thermal properties is achieved as compared to unfilled polymers. This morphology was also proven with HR-SEM pictures above in Figure 13. Depending upon the dispersion and size of the delaminated/intercalated particles some minor improvement in thermal, and marked enhancement in gas barrier properties were found. For instance, UV/VIS spectroscopy has also confirmed that transparency in the visible region was good although size of particles was still quite large compared to clay nanocomposite systems. However, despite all these improvements in both microcomposites, characterization of mechanical properties showed that poor physical interaction of the two constituents led to no improvment.

4. CONCLUSIONS

In general the addition of clay to polymers is expected to increase mechanical, thermal and gas barrier properties depending on exfoliation, intercalation and compatibility of clay particles with polymer matrix.

The attempt of preparing PS/MMT nanocomposites by melt blending method resulted in formation of either delaminated/intercalated or conventional PS/clay microcomposites containing different sizes of clay particles. Although high shear force was applied to masterbatch composites during production of the final composite materials, fully exfoliated and intercalated nanocomposite systems has not been achieved. HR-SEM pictures of the final materials verified the formation of microcomposites. The produced microcomposites, however, presented improvements in several propertis.

Thermal decomposition temperature has been improved by 20^{o}C when compared to neat PS. In comparison with virgin PS approximately 2^{o}C increase were observed in T_g values of two delaminated/intercalated PS/clay Dellite 67G and Nanofil SE 3010 microcomposites. However, decrease in T_g about 2^{o}C was obtained for conventional PS/Cloisite 11B microcomposite.

The mechanical properties have been slightly changed. No change in the Young's modulus has been obtained for PS/MMT composites compared to unfilled PS while diminishing values were observed in elongation and tensile strength at break.

Transparency has been relatively achieved in the visible region. In particular, this was proven for delaminated/intercalated microcomposites that showed 27% and 37% decrease in transmittance while conventional microcomposite had only 11% reduction in transmittance value. On the other hand, decrease in tranmittance in UV region promoted barrier resistance of composites against UV light.

Likewise, gas permeability has been reduced by about 25% and 27% for the PS/MMT microcomposites prepared with Dellite 67G and Nanofil SE 3010 respectively. This improvement in barrier property was 15% for PS/Cloisite 11B conventional microcomposite.

To conclude, there is much work to be done in order to promote exfoliation and compatibility in PS/MMT nanocomposite systems. However, the produced microcomposites investigated in this study displayed improvements in several important material properties. It is therefore concluded that an achievement of full exfoliation, compatibilization and dispersion of the clay particles in PS matrix could lead to remarkable improvements in gas barrier, thermal, mechanical and transparency properties.

5. FUTURE WORKS

This study performed herein with the aim of production of PS/clay nanocomposites with improved gas barrier, optical clarity and mechanical properties revealed the facts that there is more work that has to be done for the desired outcomes. These work can be listed as follows.

- Processing parameters can be optimized to obtain exfoliation and good dispersion of the clay particles in the PS matrix.

- New types of organo modifiers that can interact easily with PS can be used to overcome incompatibility problem between two constituents. The organo modifier should preferably have a high thermal stability that allows for processing at higher temperatures.

- HIPS can be utilized due to butadiene phase to achieve exfoliated clay structure and can be blended with the PS for better compatibility.

6. REFERENCES

[1] M. Okamoto, S. Morita, H. Taguchi, Y.H. Kim, T. Kotaka, and H. Tateyama, "Synthesis and structure of smectic clay/poly (methyl methacrylate) and clay/polystyrene nanocomposites via in situ intercalative polymerization," *Polymer*, vol. 41, 2000, pp. 3887–3890.

[2] J.E. Mark, *Physical properties of polymers handbook,* Springer, 2007.

[3] Y. Zhong, Z. Zhu, and S.Q. Wang, "Synthesis and rheological properties of polystyrene/layered silicate nanocomposite," *Polymer*, vol. 46, 2005, pp. 3006–3013.

[4] J.A. Brydson, *Plastics materials*, Butterworth-Heinemann, 1999.

[5] A.B. Strong, *Plastics: materials and processing*, 2000.

[6] V. Mittal, *Barrier properties of polymer clay nanocomposites*, Nova Science Publishers, 2010.

[7] Q.T. Nguyen and D.G. Baird, "Preparation of polymer–clay nanocomposites and their properties," *Advances in Polymer Technology*, vol. 25, 2006, pp. 270–285.

[8] B. Lepoittevin, N. Pantoustier, M. Devalckenaere, M. Alexandre, C. Calberg, R. Jérôme, C. Henrist, A. Rulmont, and P. Dubois, "Polymer/layered silicate nanocomposites by combined intercalative polymerization and melt intercalation: a masterbatch process," *Polymer*, vol. 44, 2003, pp. 2033–2040.

[9] S.J. Ahmadi, Y.D. Huang, and W. Li, "Synthetic routes, properties and future applications of polymer-layered silicate nanocomposites," *Journal of materials science*, vol. 39, 2004, pp. 1919–1925.

[10] J.M. Herrera-Alonso, Z. Sedlakova, and E. Marand, "Gas barrier properties of nanocomposites based on in situ polymerized poly (n-butyl methacrylate) in the presence of surface modified montmorillonite," *Journal of Membrane Science*, vol. 349, 2010, pp. 251–257.

[11] S. Nazarenko, P. Meneghetti, P. Julmon, B.G. Olson, and S. Qutubuddin, "Gas barrier of polystyrene montmorillonite clay nanocomposites: Effect of mineral layer aggregation," *Journal of Polymer Science Part B: Polymer Physics*, vol. 45, 2007, pp. 1733–1753.

[12] N.N. Bhiwankar and R.A. Weiss, "Melt intercalation/exfoliation of polystyrene-sodium-montmorillonite nanocomposites using sulfonated polystyrene ionomer compatibilizers," *Polymer*, vol. 47, 2006, pp. 6684–6691.

[13] R.K. Bharadwaj, "Modeling the barrier properties of polymer-layered silicate nanocomposites," *Macromolecules*, vol. 34, 2001, pp. 9189–9192.

[14] S. Su and C.A. Wilkie, "Exfoliated poly (methyl methacrylate) and polystyrene nanocomposites occur when the clay cation contains a vinyl monomer," *Journal of Polymer Science Part A: Polymer Chemistry*, vol. 41, 2003, pp. 1124–1135.

[15] S. Sinha Ray and M. Okamoto, "Polymer/layered silicate nanocomposites: a review from preparation to processing," *Progress in Polymer Science*, vol. 28, 2003, pp. 1539–1641.

[16] M. Biswas and S. Ray, "Recent progress in synthesis and evaluation of polymer-montmorillonite nanocomposites," *New polymerization techniques and synthetic methodologies*, 2001, pp. 167–221.

[17] S.W. Brindly and G. Brown, "Crystal structure of clay minerals and their X-ray diffraction," *London: Mineralogical Society*, 1980.

[18] Z. Shen, G.P. Simon, and Y.B. Cheng, "Comparison of solution intercalation and melt intercalation of polymer-clay nanocomposites," *Polymer*, vol. 43, 2002, pp. 4251–4260.

[19] N. Pantoustier, M. Alexandre, P. Degée, C. Calberg, R. Jérôme, C. Henrist, R. Cloots, A. Rulmont, and P. Dubois, "Poly (e-caprolactone) layered silicate nanocomposites: effect of clay surface modifiers on the melt intercalation process," *e-Polymers*, 2001.

[20] R.A. Vaia and E.P. Giannelis, "Polymer melt intercalation in organically-modified layered silicates: model predictions and experiment," *Macromolecules*, vol. 30, 1997, pp. 8000–8009.

[21] B. Lepoittevin, N. Pantoustier, M. Devalckenaere, M. Alexandre, D. Kubies, C. Calberg, R. Jérôme, and P. Dubois, "Poly(ε-caprolactone)/Clay Nanocomposites by in-Situ Intercalative Polymerization Catalyzed by Dibutyltin Dimethoxide," *Macromolecules*, vol. 35, Oct. 2002, pp. 8385-8390.

[22] P.C. LeBaron, Z. Wang, and T.J. Pinnavaia, "Polymer-layered silicate nanocomposites: an overview," *Applied Clay Science*, vol. 15, 1999, pp. 11–29.

[23] C. Zeng and L.J. Lee, "Poly (methyl methacrylate) and polystyrene/clay nanocomposites prepared by in-situ polymerization," *Macromolecules*, vol. 34, 2001, pp. 4098–4103.

[24] S. Su, D.D. Jiang, and C.A. Wilkie, "Novel polymerically-modified clays permit the preparation of intercalated and exfoliated nanocomposites of styrene and its copolymers by melt blending," *Polymer degradation and stability*, vol. 83, 2004, pp. 333–346.

[25] H. Li, Y. Yu, and Y. Yang, “Synthesis of exfoliated polystyrene/montmorillonite nanocomposite by emulsion polymerization using a zwitterion as the clay modifier,” *European polymer journal*, vol. 41, 2005, pp. 2016–2022.

[26] S. Advani and G. Shonaike, *Advanced Polymeric Materials*, CRC Press, 2003.

[27] J.T. Yoon, W.H. Jo, M.S. Lee, and M.B. Ko, “Effects of comonomers and shear on the melt intercalation of styrenics/clay nanocomposites,” *Polymer*, vol. 42, 2001, pp. 329–336.

[28] R.A. Vaia, H. Ishii, and E.P. Giannelis, “Synthesis and properties of two-dimensional nanostructures by direct intercalation of polymer melts in layered silicates,” *Chemistry of materials*, vol. 5, 1993, pp. 1694–1696.

[29] R.A. Vaia and E.P. Giannelis, “Lattice model of polymer melt intercalation in organically-modified layered silicates,” *Macromolecules*, vol. 30, 1997, pp. 7990–7999.

[30] A.B. Morgan and J.W. Gilman, “Characterization of polymer-layered silicate (clay) nanocomposites by transmission electron microscopy and X-ray diffraction: A comparative study,” *Journal of Applied Polymer Science*, vol. 87, Feb. 2003, pp. 1329-1338.

[31] S.T. Lim, Y.H. Hyun, H.J. Choi, and M.S. Jhon, “Synthetic biodegradable aliphatic polyester/montmorillonite nanocomposites,” *Chemistry of materials*, vol. 14, 2002, pp. 1839–1844.

[32] M. Wagner, *Thermal analysis in practice-collected applications*, Mettler Toledo Application Handbook, 2009.

[33] J. Goldstein, *Scanning electron microscopy and x-ray microanalysis*, Springer, 2003.

[34] J.Z. Zhang, *Optical properties and spectroscopy of nanomaterials*, World Scientific, 2009.

[35] V. Khrenov, M. Klapper, M. Koch, and K. M\üllen, “Surface functionalized ZnO particles designed for the use in transparent nanocomposites,” *Macromolecular Chemistry and Physics*, vol. 206, 2005, pp. 95–101.

[36] Y. Kojima, A. Usuki, M. Kawasumi, A. Okada, Y. Fukushima, T. Kurauchi, and O. Kamigaito, “Mechanical properties of nylon 6-clay hybrid,” *Journal of Materials Research*, vol. 8, 1993, pp. 1185–1189.

[37] A. Blumstein, “Polymerization of adsorbed monolayers. II. Thermal degradation of the inserted polymer,” *Journal of Polymer Science Part A: General Papers*, vol. 3, Jul. 1965, pp. 2665-2672.

[38] J. Zhu and C. Wilkie, "Flammability Properties of Polymer Nanocomposites," *Polymer Nanocomposites Handbook*, R. Gupta, E. Kennel, and K.-J. Kim, Eds., CRC Press, 2009.

[39] T. Lan, P.D. Kaviratna, and T.J. Pinnavaia, "On the nature of polyimide-clay hybrid composites," *Chemistry of Materials*, vol. 6, 1994, pp. 573–575.

[40] S. Benali, A. Olivier, P. Brocorens, L. Bonnaud, M. Alexandre, S. Bourbigot, E. Espuche, F. Gouanve, R. Lazzaroni, and P. Dubois, "Fire and Gas Barrier Properties of Poly (styrene-co-acrylonitrile) Nanocomposites Using Polycaprolactone/Clay Nanohybrid Based-Masterbatch," *Advances in Materials Science*, vol. 2008.

[41] H.W. Chen, C.Y. Chiu, and F.C. Chang, "Conductivity enhancement mechanism of the poly (ethylene oxide)/modified-clay/LiClO4 systems," *Journal of Polymer Science Part B: Polymer Physics*, vol. 40, 2002, pp. 1342–1353.

[42] P. Meneghetti and S. Qutubuddin, "Synthesis, thermal properties and applications of polymer-clay nanocomposites," *Thermochimica acta*, vol. 442, 2006, pp. 74–77.